American Society of Hematology
2021 L Street NW, Suite 900,
Washington, DC 20036
Phone: 202-776-0544 | Fax 202-776-0545
editorial@hematology.org

MiR-130b and miR-128a are essential lineage-specific co-drivers of t(4;11) MLL-AF4 acute leukemia

Tracking no: BLD-2020-006610R2

Camille Malouf (University of Edinburgh, United Kingdom) Eric Antunes (University of Edinburgh, United Kingdom) Michael O'Dwyer (University of Edinburgh, United Kingdom) Helene Jakobczyk (University of Edinburgh, United Kingdom) Franziska Sahm (University of Edinburgh, United Kingdom) Sophie-Luise Landua (University of Edinburgh, United Kingdom) Richard Anderson (University of Edinburgh, United Kingdom) Abdenour Soufi (University of Edinburgh, United Kingdom) Christina Halsey (University of Glasgow, United Kingdom) Katrin Ottersbach (University of Edinburgh, United Kingdom)

Abstract:
t(4;11) MLL-AF4 acute leukemia is one of the most aggressive malignancies in the infant and pediatric population, yet we have little information on the molecular mechanisms responsible for disease progression. This impairs the development of therapeutic regimens that can address the aggressive phenotype and lineage plasticity of MLL-AF4-driven leukemogenesis. This study highlights novel mechanisms of disease development by focusing on two microRNAs upregulated in leukemic blasts from primary patient samples: miR-130b and miR-128a. We show that miR-130b and miR-128a are downstream targets of MLL-AF4 and can individually drive the transition from a pre-leukemic stage to an acute leukemia in an entirely murine Mll-AF4 in vivo model. They are also required to maintain the disease phenotype. Interestingly, miR-130b overexpression led to a mixed/B-cell precursor/myeloid leukemia, propagated by the lymphoid-primed multipotent progenitor population, whereas miR-128a overexpression resulted in a pro-B acute lymphoblastic leukemia, maintained by a highly expanded Il7r+ckit+ blast population. Molecular and phenotypic changes induced by these two miRNAs fully recapitulate the human disease, including central nervous system infiltration and activation of an MLL-AF4 expression signature. Furthermore, we identified two downstream targets of these microRNAs, NR2F6 and SGMS1, which in extensive validation studies are confirmed as novel tumour suppressors of MLL-AF4+ leukemia. Our integrative approach thus provides a platform for the identification of essential co-drivers of MLL-rearranged leukemias, in which the pre-leukemia to leukemia transition and lineage plasticity can be dissected and new therapeutic approaches can be tested.

Conflict of interest: No COI declared

COI notes:

Preprint server: No;

Author contributions and disclosures: C.M. performed and designed experiments, analyzed the results and wrote the manuscript. E.T.B.A. and M.O.D. performed and analyzed the ATAC-Seq experiment. H.J., F.S, C.H. and S-L.L performed experiments. R.A.A. arranged clinical provision of human fetal tissues. A.S. supervised the ATAC-Seq experiment. C.H. performed the central nervous system infiltration analysis. K.O. conceived and supervised the study and wrote the manuscript.

Non-author contributions and disclosures: No;

Agreement to Share Publication-Related Data and Data Sharing Statement: The ATAC-Seq dataset has been deposited in the publicly accessible GEO repository with accession number GSE168438; emails to the corresponding author

Clinical trial registration information (if any):

MiR-130b and miR-128a are essential lineage-specific co-drivers of t(4;11) MLL-AF4 acute leukemia

Running title: MicroRNAs are key players in MLL-AF4+ leukemia

Camille Malouf[1], Eric T. B. Antunes[1*], Michael O'Dwyer[1*], Hélène Jakobczyk[1], Franziska Sahm[1], Sophie-Luise Landua[1], Richard A. Anderson[2], Abdenour Soufi[1], Christina Halsey[3], Katrin Ottersbach[1]

1 Centre for Regenerative Medicine, University of Edinburgh, UK, EH16 4UU
2 MRC Centre for Reproductive Health, The Queen's Medical Research Institute, University of Edinburgh, Edinburgh, UK. EH16 4TJ
3 Wolfson Wohl Cancer Research Centre, Institute of Cancer Sciences, University of Glasgow, Glasgow G61 1QH, UK
* These authors contributed equally.

Contact information for corresponding authors
Dr. Camille Malouf
Professor Katrin Ottersbach
Centre for Regenerative Medicine
University of Edinburgh
Edinburgh Bioquarter
5 Little France Drive
Edinburgh
EH16 4UU
UK
Tel.: +44 131 651 9516
Fax: +44 131 651 9501
camille.malouf@ed.ac.uk
katrin.ottersbach@ed.ac.uk

Word Counts
Abstract (237 words), Text (4858 words), 7 figures and 54 references
Scientific category: Lymphoid neoplasia
Key words: pediatric leukaemia, MLL-AF4, microRNA, miR-130b, miR-128a

Key points

- MiR-130b induces a Mll-AF4+ mixed/B-cell precursor/myeloid lineage acute leukemia propagated by lymphoid-primed multipotent progenitors.
- MiR-128a induces a Mll-AF4+ pro-B acute lymphoblastic leukemia propagated by Il7r+ckit+ leukemic blasts and maintained by miR-130b.

Abstract

t(4;11) MLL-AF4 acute leukemia is one of the most aggressive malignancies in the infant and pediatric population, yet we have little information on the molecular mechanisms responsible for disease progression. This impairs the development of therapeutic regimens that can address the aggressive phenotype and lineage plasticity of MLL-AF4-driven leukemogenesis. This study highlights novel mechanisms of disease development by focusing on two microRNAs upregulated in leukemic blasts from primary patient samples: miR-130b and miR-128a. We show that miR-130b and miR-128a are downstream targets of MLL-AF4 and can individually drive the transition from a pre-leukemic stage to an acute leukemia in an entirely murine Mll-AF4 in vivo model. They are also required to maintain the disease phenotype. Interestingly, miR-130b overexpression led to a mixed/B-cell precursor/myeloid leukemia, propagated by the lymphoid-primed multipotent progenitor population, whereas miR-128a overexpression resulted in a pro-B acute lymphoblastic leukemia, maintained by a highly expanded Il7r+ckit+ blast population. Molecular and phenotypic changes induced by these two miRNAs fully recapitulate the human disease, including central nervous system infiltration and activation of an MLL-AF4 expression signature. Furthermore, we identified two downstream targets of these microRNAs, NR2F6 and SGMS1, which in extensive validation studies are confirmed as novel tumour suppressors of MLL-AF4+ leukemia. Our integrative approach thus provides a platform for the identification of essential co-drivers of MLL-rearranged leukemias, in which the pre-leukemia to leukemia transition and lineage plasticity can be dissected and new therapeutic approaches can be tested.

Introduction

Acute lymphoblastic leukemia (ALL) is one of the most frequent sporadic cancers in the pediatric population.[1] The majority of patients respond well to current therapeutic regimens, but patients with t(4;11) MLL-AF4 have a dismal prognosis.[2] The development of better treatments relies on extensive knowledge of the molecular mechanisms underlying leukemogenesis. MLL-AF4+ ALL is associated with wide-spread epigenetic changes, driven and maintained by the MLL-AF4 fusion gene, that lead to the acquisition of stem cell-like features and a survival advantage.[3-7] There are few/no cooperating mutations, suggesting that MLL-AF4 alone is sufficient to drive the complete leukemogenesis process.[8]

Strong evidence supports an *in utero* origin of the disease[9,10]; yet, the recapitulation of the human disease in a syngeneic mouse model has proven challenging.[11-13] Given the prenatal origin of the disease, it is important to create a model that expresses MLL-AF4 in the physiological and genomic context of embryonic development to understand how MLL-AF4 subverts fetal hematopoiesis, as this is necessary to design new therapies specific to the aggressive infant/pediatric disease. We recently described a MLL-AF4 pre-leukemia mouse model that showed a higher self-renewal and B lymphoid bias in the Lineage-Sca1+ckit+ (LSK) compartment of the fetal liver (FL), but was missing additional factors that would allow development of a full-blown leukemia.[14-16]

MicroRNAs are essential regulators of gene expression and key modulators of hematopoiesis and leukemogenesis, but their roles in MLL-AF4-driven leukemogenesis remain elusive.[17-19] This study focuses on miR-130b and miR-128a which we found to be upregulated in MLL-AF4+ ALL patients' leukemic blasts, but which had not previously been linked to MLL-AF4+ ALL. Both are downstream targets of MLL-AF4. The overexpression of miR-130b in FL Mll-AF4+ LSK pre-leukemic cells caused a mixed/B-cell precursor (BCP)/myeloid leukemia, while miR-128a induced a pro-B ALL characterized by the expansion of Il7r+ckit+ cells. Both leukemias carried the MLL-AF4 gene expression signature, became highly penetrant and aggressive upon serial transplantation and showed central nervous system infiltration, a hallmark of the pediatric disease[20], but were propagated by different cell populations. Finally, we identified two direct targets of miR-130b and miR-128a that are downregulated in MLL-AF4+ patients (*NR2F6* and *SGMS1*) and determined that

they act as tumor suppressor genes. This study provides a novel, clinically relevant syngeneic mouse model and is an important step forward in understanding the etiology and lineage plasticity of t(4;11) MLL-AF4 leukemia.

Methods

The inducible Mll-AF4 invertor line[21] and the VEC-Cre line[22] were crossed to induce Mll-AF4 expression in definitive hematopoietic cells as described previously.[14] Detailed information regarding experimental procedures is provided in the Supplementary methods. The mouse and human ATAC-Seq files were deposited in Gene Expression Omnibus (GSE168438).

Results

MiR-130b and miR-128a are upregulated in patient blasts and have tumorigenic functions in MLL-AF4+ B-ALL cells

We obtained bone marrow (BM) aspirates of 6 infant/pediatric t(4;11) MLL-AF4 BCP ALL patients at diagnosis and remission (Supplemental Table S1) and compared the expression profile of 754 microRNAs in all MLL-AF4+ leukemic blasts at diagnosis (CD19+CD10-CD34+/-NG2+/-) to that of non-blast cells at remission (CD19-CD10-) (Figure 1A, Supplemental Figure 1A).[23] According to published studies, this non-blast population contains mostly T cells, some NK cells and HSPCs and few myeloid cells.[24,25] We included CD34 and NG2 in our sorting strategy as they are expressed on MLL-AF4+ patient blasts and leukemia-propagating cells.[26,27] We identified 66 microRNAs that are upregulated and 19 that are downregulated in patient blasts (Figure 1B, Supplemental Table S2). In support of our experimental strategy, miR-196b, which has been linked to MLL-AF4+ leukemia, showed the second highest upregulation (Supplemental Figure S1B, Supplemental Table S2).[28] Amongst the microRNAs significantly upregulated were miR-130b and miR-128a (Figure 1C,D), which have not been studied in MLL-AF4-driven leukemogenesis.

We assessed miR-130b and miR-128a expression in human hematopoietic cells (HSC, MPP, LMPP, pre-pro-B, pro-B, B/T/NK lymphoid cells, myeloid cells) and CD34- cells derived from 10-20 weeks post-conception FL (Supplemental Table S3). MiR-130b expression was significantly higher in MLL-AF4+ patient blasts compared

to human FL LMPP, pro-B, B, T and NK cells (Figure 1C), while miR-128a expression was low/absent in all FL hematopoietic cells (Figure 1D). In patient blasts, miR-128a expression was generally higher than that of miR-130b and positively correlated with a younger age of onset and a lower white blood cell count (Supplemental Figure S1B-D). MiR-130b upregulation was confined to the NG2+CD34+ and NG2-CD34+ populations (Supplemental Figure S1E), while miR-128a was similar between all three blast subtypes (Supplemental Figure S1F). In mouse tissues, miR-130b and miR-128a expression is low in normal E14 FL hematopoietic cells and in fetal and adult HSC compared to miR-126, a known HSC regulator[29] (Supplemental Figure S1G,H). This suggests that MLL-AF4+ leukemic blasts have a high expression of miR-130b and miR-128a compared to normal hematopoietic cells.

We assessed miR-130b and miR-128a promoter accessibility in one of the candidate cells-of-origin of MLL-AF4-driven leukemogenesis: human FL LMPP. Using ATAC-Seq, we revealed that miR-301b/miR-130b and miR-128a (*R3HDM1* host gene) promoters are accessible in human FL LMPP. This region is also open in MLL-AF4+ leukemic SEM cells[30] and coincides with MLL-Af4 binding in B-ALL blasts[13] (Figure 1E, Supplemental Figure S10) and MLL-AF4 in SEM cells[7] (data not shown). MiR-130b and miR-128a showed a significantly higher expression in RS4;11 and SEM MLL-AF4+ ALL cells compared to non-MLL-rearranged Nalm6 ALL and MLL/non-MLL-rearranged myeloid leukemia cell lines (Supplemental Figure S2A,B). Upon MLL-AF4 inhibition in SEM cells by a specific siRNA (siMA6) that decelerates their proliferation[31] (Supplemental Figure 2C,D), we observed a significant downregulation of MLL-AF4 and its transcriptional targets (*MEIS1*, *HOXA9*, *CDK6*, *BCL2*), as well as miR-130b and miR-128a (Figure 1F,G). These results highlight two new MLL-AF4 target genes: miR-130b and miR-128a.

To gain an initial insight into their importance in MLL-AF4+ leukemia, we stably inhibited the activity of miR-130b and miR-128a in human leukemia cell lines using commercially available short hairpin RNA (pmiRZip). MiR-130b or miR-128a single inhibition reduced SEM and RS4;11 cell proliferation (Figure 1H, Supplemental Figure S2E). Strikingly, miR-130b and miR-128a dual inhibition led to a massive increase in SEM cell death (Figure 1I), while RS4;11 cells were more sensitive to miR-130b single inhibition (Supplemental Figure S2F).

We also verified the disease-propagating potential of SEM cells transplanted into NSG mice upon miRNA inhibition. SEM pmiRZip-130b-engrafted NSG mice had a significantly longer survival (81 days) compared to SEM control- or pmiRZip-128a-engrafted NSG mice (58 days) (Figure 1J). This striking difference could be partly due to the long-term and maintained downregulation of miR-128a in SEM pmiRZip-130b cells (Supplemental Figure 2G), whereas SEM control and pmiRZip-128a cells have similar expression of miR-130b (Supplemental Figure 2H). SEM pmiRZip-130b-engrafted NSG mice had diminished splenohepatomegaly and engraftment in peripheral blood and liver (Supplemental Figure 2I,J). Finally, miR-130b inhibition decreased the proportion of SEM cells that express the CD33 myeloid marker whereas miR-128a inhibition increased CD33 positivity (Supplemental Figure S2L). These data suggest that miR-130b and miR-128a affect the survival and lineage plasticity of B-ALL leukemia cells and led us to investigate their role in MLL-AF4+ leukemogenesis, starting at the pre-leukemia stage in our mouse model.[14]

MiR-130b and miR-128a promote B-lymphoid bias of FL Mll-AF4+ pre-leukemic cells

We detected low/intermediate expression of miR-130b and miR-128a in murine FL HSC/MPP and LMPP (Figure 2A), from which MLL-AF4+ leukemia is thought to originate.[14,15,32] This expression pattern remains stable upon Mll-AF4 induction, suggesting that the overexpression seen in patients is not recapitulated in pre-leukemic mice. We investigated chromatin accessibility in mouse FL LMPP (WT and Mll-AF4+ VEC-Cre+) by ATAC-Seq (Figure 2B) and revealed that the miR-301b/miR-130b and miR-128a (*R3hdm1* host gene) promoters displayed similar accessibility to that seen in human cells (Figure 1E); however, the accessibility of these promoters decreased upon Mll-AF4 expression. This is in line with the absence of Mll-AF4-induced upregulation of miR-130b and miR-128a expression in mouse FL cells (Figure 2A). Thus, we overexpressed each microRNA individually in FL LSK cells, which contain HSC/MPPs and LMPPs, from control (Mll-AF4- VEC-Cre+) and Mll-AF4+ (Mll-AF4+ VEC-Cre+) mice and carried out functional validation (Figure 2C-E). In colony-forming assays, miR-130b overexpression maintained the myeloid clonogenic potential of Mll-AF4+ FL LSK while miR-128a decreased it (Figure 2F). Both microRNAs increased the B-lymphoid clonogenic potential (Figure 2G). MiR-130b also increased cell proliferation in myeloid conditions, while miR-128a

increased proliferation in B-lymphoid conditions (Figure 2H). These effects were specific to Mll-AF4+ cells, but did not lead to immortalization *in vitro* (Supplemental Figure S2M,N). These results indicate that miR-130b and miR-128a enhance the Mll-AF4-mediated hematopoietic clonogenic potential *in vitro*, especially of the B-lymphoid lineage.

The overexpression of miR-130b and miR-128a in Mll-AF4+ FL LSK leads to a mixed/BCP/myeloid or pro-B lymphoblastic acute leukemia, respectively

To assess the consequences of miR-130b or miR-128a overexpression in MLL-AF4-driven leukemogenesis, we transplanted transduced/GFP+ FL Mll-AF4+ LSK and monitored primary recipients for 18 months (Figure 3A). Detailed post-mortem analysis is included (Supplemental Table S4,5). Only 1/15 primary recipients from the control cohort (FL Mll-AF4+ LSK pMIRH/pmiRZip-scramble) developed a hematological malignancy with enlarged spleen and an expansion of mature B-lymphoid cells, but the GFP chimerism decreased upon serial transplantation (Supplemental Figure S3A,B). Similar to previous studies, this suggests an incomplete transformation.[14-16] 5/7 FL Mll-AF4+ LSK pMIRH-130b primary recipients and 5/9 FL Mll-AF4+ LSK pMIRH-128a primary recipients developed a hematological malignancy with splenohepatomegaly and pale bones (Figure 3B,C, Supplemental Table S4).

To assess the transformation of GFP+ cells of pMIRH-130b and pMIHR-128a sick mice, we performed secondary/tertiary transplantations of total BM from sick mice that harbored an immature B-lymphoid phenotype (mixed/BCP/myeloid or pro-B) (Figure 3D). Mice with a myeloid disease showed weak transformation through serial transplantation as the vast majority of recipients remained disease-free (data not shown), which corroborates with MLL-AF4 being more potent in a B-lymphoid context.[13,33] All secondary/tertiary recipients in pMIRH-130b and pMIRH-128a cohorts developed a hematological malignancy (Figure 3B,C). The latency became significantly shorter, suggesting progressing aggressiveness. Sick mice suffered from splenohepatomegaly, pale bones and their BM contained close to 100% GFP+ cells (Figure 3E-H). pMIRH-130b sick mice also presented with an elevated white blood cell count (Figure 3I) and decreased platelet/red blood cell counts (Supplemental Figure S3C,D). GFP+ cells also invaded the peripheral blood, spleen, liver and lung (Supplemental Figure S3F-I).

We next analyzed the cell surface phenotype of GFP+ cells in the BM. In addition to a slight increase in B220-CD11b+Gr1+ myeloid cells, pMIRH-130b sick mice showed a striking expansion of mixed lineage cells (Figure 3J,K). These populations were absent in pMIRH-128a sick mice. pMIRH-130b sick mice had expanded B220+CD19- immature B-cells at the expense of B220+CD19+ B-cells, which were also lost in pMIRH-128a sick mice (Figure 3L). The T-cell compartment was reduced/absent in pMIRH-128a sick mice (Supplemental Figure 3E). Hence, miR-128a arrested the maturation of all blood lineages and all GFP+ cells were ckit+IgM-Il7r+ (Figure 3M,N). All hematopoietic phenotypes were recapitulated in the peripheral blood, spleen, liver and lung (Supplemental Figure S3F-I). Finally, we detected an increase in Flt3+ and Sca1+ cells in pMIRH-130b and pMIRH-128a sick mice, respectively (Supplemental Figure S3J,K). This increased the LSK and Lineage-ckit+/common lymphoid progenitor (LK/CLP) compartments in pMIRH-128a sick mice, suggesting that GFP+ cells maintained their stem-cell phenotype and were completely blocked at the pro-B stage (Supplemental Figure S3L,M). While the LSK compartment in pMIRH-128a sick mice was almost 100% Il7r+Flt3- in all recipients, we observed an increase in the LMPP fraction upon serial transplantation in pMIRH-130b sick mice (Figure 3O).

One of the hallmarks of t(4;11) MLL-AF4 BCP-ALL is infiltration of the central nervous system by leukemic blasts.[20,34] This was absent in control mice, but pMIRH-130b and especially pMIRH-128a sick mice showed significant blast infiltration in the leptomeninges (Figure 3P). We detected cells with a blast appearance in the peripheral blood, BM and spleen of pMIRH-130b and pMIRH-128a sick mice (Figure 3Q, Supplemental Figure S3N). Overall, the individual overexpression of miR-130b or miR-128a in Mll-AF4+ FL LSK caused hematological malignancies with all the phenotypic features seen in MLL-AF4+ leukemia patients.

Mll-AF4+ pMIRH-130b/pMIRH-128a+ cells display a gene expression profile similar to MLL-AF4+ patient blasts

To further characterize the phenotype, we conducted gene expression analyses of key players in MLL-AF4+ leukemogenesis (Supplemental Table S6) in pre-leukemia cells (transduced/GFP+ FL Mll-AF4+ LSK pre-transplantation) and Mll-AF4+ BM cells (control/pMIRH, pMIRH-130b/128a sick mice).[15,35-38] At the pre-leukemia stage, miR-130b and miR-128a overexpression led to an upregulation of

Mll-AF4 (Figure 4A) and components of the Mll-AF4 transcriptional machinery (*Mll*, *Af4, Ledgf, Ccnt1, Zfp64, Brd4*), resulting in a significant upregulation of *Flt3, Hoxa9* and *Lmo2* (Figure 4B,C). *E2a* was also upregulated, which partly explains the increased B-lymphoid clonogenic potential (Figure 4B,C, 2G). *Cdk9* was upregulated in the presence of miR-130b, while miR-128a caused downregulation of *Gsk3b* and upregulation of *Cdk6* and *Pax5* (Figure 4B,C).

Mll-AF4 was detected in pMIRH-130b and pMIRH-128a sick mice, but no longer in control mice (Figure 4D). As disease progresses, BM cells of all sick mice maintained a significantly higher expression of *Ccnt1*, *Cdk9*, *Dot1l, Brd4* and a decreased expression of *Zfp64* (Figure 4E,F). pMIRH-130b sick mice upregulated *Flt3*, *Hoxa9*, *Cdk6* and *Bcl2*, while pMIRH-128a sick mice upregulated *Meis1*, *Runx1*, *Cdk6* and *Bcl2* (Figure 4E,F). This suggests that both microRNAs promote the expression of essential components of the Mll-AF4 transcriptional machinery and their target genes. Other B-lineage associated genes (*Pax5, Il7r, Ikaros*) were also upregulated in sick mice, which correlates with the lineage association of the hematological malignancies (Figure 4E,F, 3).

We also confirmed the expression of miR-130b and miR-128a in sick mice, and three microRNAs downregulated in patients (miR-99b, miR-125a-5p, miR-194) (Figure 4E,F, Supplemental Table S2). pMIRH-130b sick mice showed an overexpression of miR-130b, miR-99b and miR-194, while pMIRH-128a sick mice had a microRNA expression profile more similar to patient leukemic blasts: miR-130b and miR-128a upregulation; miR-99b, miR-125a-5p and miR-194 downregulation.

Finally, we verified the expression of miR-130b and miR-128a target genes linked to leukemogenesis and/or B-cell development. MiR-130b and miR-128a expression led to an upregulation of *Creb1*, *Marcks*, *Jarid2* and *Lcor* at the pre-leukemia stage (Supplemental Figure 4A,B). MiR-128a also caused an upregulation of *Mllt10*, which interacts with DOT1L to mediate H3K79 dimethylation (Supplemental Figure 4A,B).[39] With the establishment of the disease and similar to patients, *Brwd1*, *Creb1* and *E2f3* became upregulated in pMIRH-130b and pMIRH-128a sick mice, as well as *Bmi1*, *Brwd3*, *Mllt10* and *Pten* in pMIRH-128a sick mice (Supplemental Figure 4C,D). Brwd1 promotes B-lymphopoiesis through RAG recruitment[40], while BMI1 is important for MLL-rearranged leukemia maintenance.[41] Finally, in line with bortezomid-sensitivity of MLL-AF4+ leukemic cells, miR-130b led to a significant downregulation of *Marcks*, a protein kinase C substrate associated

with bortezomid resistance (Supplemental Fig. 4C,D).[42,43] Overall, 35/40 genes (88%) had an expression pattern similar between infant/pediatric patients and sick mice. Therefore, the expression pattern observed in sick mice largely recapitulates that of MLL-AF4+ BCP ALL.

MiR-130b+ and miR-128a+ Mll-AF4+ leukemia is propagated by different LSCs

Our previous studies have pointed to the FL LMPP as the most likely cell-of-origin of t(4;11) MLL-AF4 ALL.[14,15] pMIRH-130b sick mice also showed an increased LMPP compartment upon serial transplantation (Figure 3). To determine which population contains leukemia-propagating/stem cells, we individually transplanted HSC/MPPs, LMPPs, LK/CLPs and LSK Il7r+ (pMIRH-128a only) from the BM of sick mice to assess their ability to transfer the disease (Figure 5A). 2/3 mice that received 100 LMPPs from pMIRH-130b primary/sick mouse showed engraftment and overt disease after a latency of only 41 days, while there was no contribution from injected HSC/MPPs and LK/CLPs (Figure 5B). As the disease became more aggressive with serial transplants, a low number of HSC/MPP or LMPP (and high number of LK/CLP) from pMIRH-130b secondary/sick mice was sufficient to phenocopy the leukemia in tertiary recipients (Figure 5C).

Interestingly, we did not observe an engraftment from the few retrieved HSC/MPP and LMPP from primary/sick or secondary/sick pMIRH-128a mice. Leukemia-propagating ability was restricted to the blast populations (LK/CLP and LSK Il7r+ fractions) in pMIRH-128a sick mice (Figure 5D,E). The GFP chimerism in the BM of secondary and tertiary recipients was >85% in sick mice (Figure 5F,G)

Secondary/sick recipients of LMPP from pMIRH-130b primary/sick mice showed splenohepatomegaly, pale bones and a mixed/BCP/myeloid lineage phenotype (Figure 5H,I, Supplemental Table S4). Faithful disease propagation was also confirmed in tertiary recipients of both pMIRH-130b and pMIRH-128a sorted cells (Figure 5I-M, Supplemental Figure S5). The LSK compartment of pMIRH-130b tertiary/sick mice was largely dominated by the LMPP population, whether mice received HSC/MPP or LMPP (Figure 5N). This confirms that LMPPs propagate the mixed/BCP/myeloid lineage acute leukemia observed in pMIRH-130b mice, whereas the Lineage-Sca1+/-Il7r+ckit+ blast population maintains the pro-B ALL in pMIRH-128a mice.

NR2F6 and SGMS1, two targets of miR-130b and miR-128a, have tumor suppressor activity

To identify the downstream mechanisms of miR-130b and miR-128a, we intersected the differentially expressed genes that are common between pediatric and infant MLL-AF4+ leukemia with predicted targets of miR-130b and miR-128a (Figure 6A).[38,44-46] We selected *NR2F6* (miR-128a target) and *SGMS1* (miR-130b and miR-128a target) for functional validation given their unknown role in MLL-AF4+ leukemia. NR2F6 is a transcriptional repressor with predicted DNA-binding sites in the *MLL* promoter, whereas SGMS1 synthesizes sphingomyelin which is an essential component of the plasma membrane.[47] Both genes are downregulated in MLL-AF4+ leukemia patients (Figure 6B,C, Supplemental Figure S6A-D) and in MLL-rearranged leukemia cell lines compared to Nalm6 cells (Supplemental Figure S6E,F). We also observed their downregulation in pMIRH-130b and pMIRH-128a leukemic mice (Figure 6D,E).

To establish a direct link between miR-130b/miR-128a and NR2F6/SGMS1 in human MLL-AF4+ leukemic cells, we used specific siRNAs against miR-130b or miR-128a to inhibit their activity in SEM cells. Both induced a decelerated cell proliferation (Supplemental Figure S6G), which correlates with SEM proliferation upon inhibition with pmiRZip (Figure 1H). MiR-130b or miR-128a inhibition in SEM cells initiated a strong downregulation of miR-130b, miR-128a, *MLL-AF4* and its transcriptional targets (*MEIS1*, *HOXA9*, *CDK6*, *BCL2*), and, importantly, strongly upregulated *NR2F6* and *SGMS1* at the transcript and protein level (Figure 6F,G). This was recapitulated with MLL-AF4 inhibition through siMA6 (Supplemental Figure S6H,I) and in SEM pmiRZip-130b cells, which maintained a long-term miR-128a downregulation (Supplemental Figure S6J,K). Finally, using a luciferase assay, we observed a significant decrease in luciferase activity when miR-128a is overexpressed alongside the pGL3promoter-UTR-NR2F6 or pGL3promoter-UTR-SGMS1 in HEK293T cells (Supplemental Figure S6L). The effect was similar, but weaker, when miR-130b was overexpressed with the pGL3promoter-UTR-SGMS1 (Supplemental Figure S6M).

To assess the role of NR2F6 and SGMS1 in human MLL-AF4+ leukemic cells, we overexpressed them in SEM and RS4;11 leukemic cells (Supplemental Figure S6N,O). SGMS1 overexpression in SEM cells led to increased cell death (Figure 6H), while NR2F6 significantly decreased cell proliferation (Figure 6I). These effects

were recapitulated in RS4;11 leukemia cells (Supplemental Figure S6P,Q). Furthermore, NR2F6 overexpression in SEM cells was linked to a downregulation of *MLL-AF4* and its target genes *(MEIS1*, *HOXA9*, *BCL2,* miR-130b, miR-128a) (Figure 6J). We also observed a prolonged survival of SEM-pCDH-hNR2F6-engrafted NSG mice of up to 64 days after transplant (Figure 6K). Overall, these results identified a direct link between miR-130b/miR-128a and NR2F6/SGMS1, which promotes MLL-AF4+ leukemia maintenance.

Continued miR-130b activity and NR2F6/SGMS1 inhibition are required for MLL-AF4+ leukemia.

To confirm the crucial role of miR-130b, miR-128a, NR2F6 and SGMS1 in MLL-AF4+ leukemia maintenance, we conducted rescue experiments using the pmiRZip microRNA inhibitors and NR2F6 and SGMS1 overexpression. A summary of the rescue mouse cohort is included (Supplemental Table S7). GFP+ leukemic cells from pMIRH-130b sick/secondary recipients were transduced with a control inhibitor (pmiRZip-scramble), an anti-miR-130b (pmiRZip-130b), a NR2F6 vector (pCDH-hNR2F6) or a SGMS1 vector (pCDH-hSGMS1) and transplanted (Figure 7A). MiR-130b inhibition and *NR2F6*/*SGMS1* upregulation were confirmed in Mll-AF4+ pMIRH-130b pmiRZip-130b pre-transplant and BM cells (Supplemental Figure S7A). We also confirmed *NR2F6* and *SGMS1* overexpression in pre-transplant and BM cells of Mll-AF4+ pMIRH-130b pCDH-hNR2F6 and pCDH-hSGMS1, while miR-130b expression was stable (Supplemental Figure S7A). MiR-130b inhibition and NR2F6 overexpression led to a significantly prolonged latency compared to control mice (53 and 62 vs 23 days, respectively) (Figure 7B). SGMS1 overexpression was not able to maintain Mll-AF4+ pMIRH-130b leukemia and led to a stroke-like phenotype in all recipients (Figure 7B, Supplemental Table S7). While Mll-AF4+ pMIRH-130b pCDH-hSGMS1 rescue mice presented a significantly lower blast infiltration in all tissues and no splenohepatomegaly, Mll-AF4+ pMIRH-130b pmiRZip-130b and pCDH-hNR2F6 rescue mice eventually developed leukemia (Figure 7C, Supplemental Figure S7B,C) Mll-AF4+ pMIRH-130b rescue mice displayed a reduced contribution from the myeloid compartment and an increased contribution from mixed lineage cells (Figure 7D, Supplemental Figure S7D-G). B-lymphoid cells, including committed B220+CD19+ cells were also restored in Mll-AF4+ pMIRH-130b rescue mice (Figure 7D, Supplemental Figure S7D-G), suggesting that miR-130b mediates

the B-lymphoid differentiation arrest through the downregulation of NR2F6 and SGMS1.

Secondly, given miR-130b upregulation in the BM of pMIRH-128a sick mice (Figure 4E), we performed single or double inhibition of miR-128a and miR-130b and NR2F6/SGMS1 overexpression in GFP+ leukemic cells from pMIRH-128a sick/secondary recipients (Figure 7A). The single or double inhibition of miR-128a and miR-130b led to a downregulation of both miR-130b and miR-128a in Mll-AF4+ pMIRH-128a pre-transplant cells (Supplemental Figure S7H), which is similar to what has been observed in SEM cells (Figure 6F). This miR-130b/miR-128a inhibition was accompanied by an upregulation of *NR2F6* and *SGMS1* (Supplemental Figure S7H). Similar to the results with SEM cells (Figure 1J), miR-128a inhibition did not affect disease latency (Figure 7E), suggesting that miR-128a inhibition is more important for the initiation of MLL-AF4-driven leukemogenesis. Strikingly, miR-130b inhibition led to a total rescue of 50% of recipients, highlighting a critical role for pro-B ALL maintenance (Figure 7E). MiR-128a and miR-130b dual inhibition led to a similar rescue phenotype and a longer latency (Figure 7E). Similar to Mll-AF4+ pMIRH-130b rescue mice, NR2F6 overexpression showed a trend towards a longer latency ($p = 0.08$) and SGMS1 induced a stroke-like phenotype (Figure 7F). MiR-130b inhibition alone or with pmiRZip-128a as well as NR2F6/SGMS1 overexpression reduced splenohepatomegaly (Supplemental Figure S7I,J) and all showed a significantly decreased GFP chimerism in the BM (Figure 7G,H). The GFP chimerism in the peripheral blood, spleen, liver and lungs was also reduced in some rescue mice (Figure S7K-N). Finally, similar to SEM cells (Figure 6H), SGMS1 overexpression in Mll-AF4+ pMIRH-130b and Mll-AF4+ pMIRH-128a mice increased mouse leukemic blast cell death in the BM, peripheral blood, spleen, liver and lungs (Figure 7I, Supplemental Figure S7O-R). This may cause an accumulation of debris in vessels/arteries, leading to blockages which could explain the stroke-like phenotype observed in SGMS1 rescue mice. NR2F6 overexpression also decreased the viability of mouse leukemic cells, which correlated with the longer latency observed in recipients (Figure 7B,F).

All pre-transplant cells transduced with a microRNA inhibitor or overexpressing gene showed a downregulation of Mll-AF4 and some of its target genes (Supplemental Figure S7A,H). This Mll-AF4 downregulation was also seen in the BM of rescue mice, but was not necessarily linked to a downregulation of Mll-

AF4 target genes such as *Meis1*, *Hoxa9*, *Cdk6* or *Bcl2*. We also observed a partial/full recovery of *Nr2f6* and *Sgms1* expression following miR-130b inhibition in pMIRH-130b and pMIRH-128a leukemic mice (Supplemental Figure S8).

In contrast to the rescue phenotype observed in sick mice, NR2F6 or SGMS1 overexpression in mouse Mll-AF4+ pre-leukemic cells impaired engraftment and did not lead to the stroke-like phenotype caused by SGMS1 overexpression in sick mice (Supplemental Figure S9A-E). SGMS1 also favored the production of B220+ CD19+ B-lymphoid cells, which can partially be explained by *Pax5* upregulation (Supplemental Figure S9F-I).

These results confirm that the phenotype observed in our sick mice is microRNA-dependent and mediated through NR2F6 and SGMS1 downregulation. We also highlight their distinct biological roles in the initiation and maintenance of MLL-AF4-driven leukemogenesis and show that both NR2F6 and SGMS1 are tumor suppressor genes in MLL-AF4-driven leukemogenesis (Supplemental Figure S11). These represent attractive targets for future studies that will focus on the identification of new therapeutic avenues for MLL-AF4+ leukemia.

Discussion

Our aim was to improve the understanding of MLL-AF4+ leukemogenesis and to find collaborating factors that could serve as new therapeutic targets. We focused on miR-130b and miR-128a for functional validation because of their strong upregulation in MLL-AF4+ BCP-ALL patient leukemic blasts from our and published cohorts.[48] We used an integrative approach using human leukemic cell lines and a pre-leukemia mouse model of t(4;11) MLL-AF4 ALL with physiological expression levels of Mll-AF4 in the correct cellular context[14,15], as this model would allow for the identification of factors that drive the pre-leukemic state to a full acute leukemia phenotype.

MiR-130b and miR-128a, which we identified as two novel downstream targets of MLL-AF4, were not overexpressed in the Mll-AF4 pre-leukemia mouse model.[14] ATAC-Seq showed similar accessibility of the two loci in wild-type mouse and human FL LMPPs, which decreased upon Mll-AF4 expression in mouse cells. This was unexpected, but may be due to key members of the MLL-AF4 complex not being expressed in mouse progenitors. For this reason, we decided to overexpress the two miRNAs separately to assess their individual contribution to disease development. The overexpression of miR-130b or miR-128a in FL Mll-AF4+ LSK enhanced B-lymphoid clonogenic output, and most importantly, a significant subset of FL Mll-AF4+ LSK miR-130b+ or miR-128+ primary recipients developed an acute leukemia with similar phenotypic and molecular features as seen in patients. Specifically, Mll-AF4 and miR-130b together drove a progressively more severe mixed/BCP/myeloid lineage acute leukemia characterized by an expansion of B220+ mixed lineage, BCP and myeloid cells. The combination of Mll-AF4 and miR-128a induced an acute leukemia with shortening latency over serial transplants and a phenotype that resembled that of pro-B cells (Lin-ckit+Il7r+). B220 and CD19 expression was lacking, but B-lymphoid associated genes were expressed (*Ikaros* and *Pax5*). Therefore, miR-128a induced a very strong B-lymphoid differentiation arrest, with a lack of IgM-expressing mature B cells, and an upregulation of ckit and Sca1 stem cell markers. There was also a strong upregulation of miR-130b in Mll-AF4+ miR-128a sick mice.

This mouse model enables the comparison of gene expression at the pre-leukemia and leukemia stages, which is impossible to achieve with human samples

because of the pre-natal origin of t(4;11) MLL-AF4 acute leukemia. Already at the pre-leukemic stage, the expression of miR-130b or miR-128a increased the expression of *Mll-AF4* and key players in Mll-AF4+ leukemogenesis that can explain some of the phenotypic differences observed in the sick mice (mixed/BCP/myeloid versus pro-B ALL). We observed a strong overlap with the expression signature in patients, including maintenance of Mll-AF4 expression. Hence, a full leukemic phenotype was achieved in a syngeneic mouse model with only one additional co-driver. Furthermore, with the rescue experiments highlighting the differential roles of miR-130b and miR-128a in leukemia progression and lineage identity, future experiments will focus on identifying the factors that modulate miR-130b and miR-128a expression and that are absent in mice.

Patients with t(4;11) MLL-AF4 leukemia present with an expansion of leukemic blasts that have a phenotype similar to pro-B cells (CD19+CD10-) and retain myeloid features (CD15+), and myeloid leukemic clones can emerge during disease progression.[49 50] This suggests that the cell-of-origin of t(4;11) MLL-AF4 B-ALL retains lymphoid and myeloid potential, which could explain the “lineage switch” observed in some patients following treatment.[51-53] In Mll-AF4+ miR-130b+ mice, we also observed a co-expression of myeloid and lymphoid markers on a substantial proportion of leukemic cells. Furthermore, LMPPs, which retain both myeloid and lymphoid potential and became the prominent LSC population as disease progressed, were able to recapitulate the mixed/BCP/myeloid lineage acute leukemia.

The leukemia-propagating cell in Mll-AF4+ miR-128a+ sick mice was very different. Almost all of the cells in the LSK and LK/CLP compartment in these mice expressed Il7r, and the few HSC/MPP and LMPP retrieved from their BM did not engraft. Only the ckit+Il7r+Sca1+/- blast cells from Mll-AF4+ miR-128a+ sick mice propagated pro-B ALL, with both fractions yielding Sca1- and Sca1+ in sick mice (data not shown), a pattern observed with other markers in BCP-ALL patient samples (e.g. CD34).[27,54]

Extensive functional validation in human and mouse cells has highlighted the importance of miR-130b upregulation in the initiation and maintenance of MLL-AF4+ acute leukemia. Even though miR-130b expression was detected in normal pre-pro-B human FL cells, this study confirms that MLL-AF4 is important to drive and/or maintain miR-130b upregulation. Finally, we identified two novel tumor suppressor

genes, *NR2F6* and *SGMS1,* that are downregulated in t(4;11) MLL-AF4 ALL patients and confirmed that they are direct targets of miR-130b and miR-128a. Their individual overexpression strongly compromised the proliferation and survival of MLL-AF4+ lymphoid human leukemic cells. In Mll-AF4+ miR-130b+ and Mll-AF4+ miR-128a+ leukemic mice, *NR2F6* and *SGMS1* led to prolonged latency, less severe/absent splenohepatomegaly and compromised leukemic blast infiltration and viability. Future work will focus on refining our understanding of the mechanisms modulated by these genes for therapeutic use. Results from this study highlight a strong apoptotic and toxic response upon SGMS1 overexpression that is specific to Mll-AF4+ leukemic cells compared to Mll-AF4+ pre-leukemic cells. Hence, it will be essential to carefully control SGMS1 activity for clinical use to reduce the risk of severe complications for patients. Furthermore, if MLL is a direct target of the NR2F6 transcription repressor, the identification of molecules that can activate its ligand-binding-domain could prove useful to target MLL-AF4 activity in leukemic cells.

This study provides new mouse models of t(4;11) MLL-AF4 acute leukemia with different lineage phenotypes. These are important tools for the development of better therapeutic regimens and for investigating lineage choice in MLL-rearranged leukemias. Our integrative approach can validate the role of leukemogenic co-drivers in a physiological context and allows, for the first time, to study every stage of the disease, from the pre-leukemia stage to MLL-AF4+ leukemia.

Acknowledgements

This study was supported by a Blood Cancer UK Bennett Senior Fellowship (K.O.) and grants from the Kay Kendall Leukaemia Fund (K.O.) and Cancer Research UK (K.O., E.T.B.A.). The work was also supported by an MRC career development award (MR/N024028/1) (A.S) and a Ph.D scholarship from the Darwin Trust of Edinburgh (M.O.D). The authors are extremely grateful to patients, their parents and the Blood Cancer UK Childhood Leukaemia Cell Bank for providing MLL-AF4+ samples. The authors would also like to thank Fiona Rossi, Andrea Corsinotti, Claire Cryer and Bindy Heer from the CRM Flow Cytometry Facility for cell sorting services and flow cytometry advice, Clare Orange and Lynn Stevenson, University of Glasgow, for the brain histology and imaging and Bertrand Vernay and Mathieu Vermeren from the CRM Imaging Facility. We are especially grateful to patients for donating fetal tissue and A. Saunderson and N. Forson for obtaining consent from patients and collecting specimens. We are very grateful to Prof. Thomas Milne for helpful comments on the manuscript. We acknowledge the support of James Todd, Andrew Dyer, Allan Booth, Hollie McGrath, Linda Dunn-Campbell, Jacek Mendrychowski, Stephen Henretty, John Agnew, Stuart Fleming and Jamie Kelly from the CRM Animal Facility in animal experimentation. Core facilities at the Edinburgh Centre for Regenerative Medicine are supported by centre grant MR/K017047/1. Some work was carried out at the MRC Centre for Reproductive Health, supported by MRC grants G1100357 and MR/N022556/1.

Authorship Contributions

C.M. performed and designed experiments, analyzed the results and wrote the manuscript. E.T.B.A. and M.O.D. performed and analyzed the ATAC-Seq experiment. H.J., F.S, C.H. and S-L.L performed experiments. R.A.A. arranged clinical provision of human fetal tissues. A.S. supervised the ATAC-Seq experiment. C.H. performed the central nervous system infiltration analysis. K.O. conceived and supervised the study and wrote the manuscript.

Conflicts of Interest disclosure

The authors have no conflicts of interest to disclose.

References

1. Ward E, DeSantis C, Robbins A, Kohler B, Jemal A. Childhood and adolescent cancer statistics, 2014. *CA: A Cancer Journal for Clinicians*. 2014;64(2):83-103.
2. Schrappe M, Hunger SP, Pui C-H, et al. Outcomes after Induction Failure in Childhood Acute Lymphoblastic Leukemia. *New England Journal of Medicine*. 2012;366(15):1371-1381.
3. Krivtsov AV, Feng Z, Lemieux ME, et al. H3K79 Methylation Profiles Define Murine and Human MLL-AF4 Leukemias. *Cancer Cell*. 2008;14(5):355-368.
4. Wang Z, Smith KS, Murphy M, Piloto O, Somervaille TCP, Cleary ML. Glycogen synthase kinase 3 in MLL leukaemia maintenance and targeted therapy. *Nature*. 2008;455(7217):1205-1209.
5. Dawson MA, Prinjha RK, Dittmann A, et al. Inhibition of BET recruitment to chromatin as an effective treatment for MLL-fusion leukaemia. *Nature*. 2011;478(7370):529-533.
6. Godfrey L, Crump NT, O'Byrne S, et al. H3K79me2/3 controls enhancer–promoter interactions and activation of the pan-cancer stem cell marker PROM1/CD133 in MLL-AF4 leukemia cells. *Leukemia*. 2020.
7. Kerry J, Godfrey L, Repapi E, et al. MLL-AF4 Spreading Identifies Binding Sites that Are Distinct from Super-Enhancers and that Govern Sensitivity to DOT1L Inhibition in Leukemia. *Cell Reports*. 2017;18(2):482-495.
8. Andersson AK, Ma J, Wang J, et al. The landscape of somatic mutations in infant MLL-rearranged acute lymphoblastic leukemias. *Nat Genet*. 2015;47(4):330-337.
9. Gale KB, Ford AM, Repp R, et al. Backtracking leukemia to birth: Identification of clonotypic gene fusion sequences in neonatal blood spots. *Proceedings of the National Academy of Sciences of the United States of America*. 1997;94(25):13950-13954.
10. Greaves M. In utero origins of childhood leukaemia. *Early Human Development*. 2005;81(1):123-129.
11. Malouf C, Ottersbach K. Molecular processes involved in B cell acute lymphoblastic leukaemia. *Cellular and Molecular Life Sciences*. 2017;75(3):417-446.
12. Milne TA. Mouse models of MLL leukemia: recapitulating the human disease. *Blood*. 2017;129(16):2217-2223.
13. Lin S, Luo Roger T, Ptasinska A, et al. Instructive Role of MLL-Fusion Proteins Revealed by a Model of t(4;11) Pro-B Acute Lymphoblastic Leukemia. *Cancer Cell*. 2016;30(5):737-749.
14. Barrett Neil A, Malouf C, Kapeni C, et al. Mll-AF4 Confers Enhanced Self-Renewal and Lymphoid Potential during a Restricted Window in Development. *Cell Reports*. 2016;16(4):1039-1054.
15. Malouf C, Ottersbach K. The fetal liver lymphoid-primed multipotent progenitor provides the prerequisites for the initiation of t(4;11) MLL-AF4 infant leukemia. *Haematologica*. 2018;103(12):e571-e574.
16. Malouf C, Ottersbach K. Fetal liver Mll-AF4+ hematopoietic stem and progenitor cells respond directly to poly(I:C), but not to a single maternal immune activation. *Experimental Hematology*. 2019;76:49-59.
17. Chung SS, Hu W, Park CY. The Role of MicroRNAs in Hematopoietic Stem Cell and Leukemic Stem Cell Function. *Therapeutic Advances in Hematology*. 2011;2(5):317-334.
18. MacFarlane L-A, Murphy PR. MicroRNA: Biogenesis, Function and Role in Cancer. *Current Genomics*. 2010;11(7):537-561.
19. Yendamuri S, Calin GA. The role of microRNA in human leukemia: a review. *Leukemia*. 2009;23(7):1257-1263.
20. Williams MTS, Yousafzai YM, Elder A, et al. The ability to cross the blood–cerebrospinal fluid barrier is a generic property of acute lymphoblastic leukemia blasts. *Blood*. 2016;127(16):1998-2006.
21. Metzler M, Forster A, Pannell R, et al. A conditional model of MLL-AF4 B-cell tumourigenesis using invertor technology. *Oncogene*. 2006;25(22):3093-3103.
22. Chen MJ, Yokomizo T, Zeigler B, Dzierzak E, Speck NA. Runx1 is required for the endothelial to hematopoietic cell transition but not thereafter. *Nature*. 2009;457(7231):887-891.

23. Dvinge H, Bertone P. HTqPCR: high-throughput analysis and visualization of quantitative real-time PCR data in R. *Bioinformatics*. 2009;25(24):3325-3326.
24. Witkowski MT, Dolgalev I, Evensen NA, et al. Extensive Remodeling of the Immune Microenvironment in B Cell Acute Lymphoblastic Leukemia. *Cancer Cell*. 2020;37(6):867-882.e812.
25. Rouce RH, Shaim H, Sekine T, et al. The TGF-β/SMAD pathway is an important mechanism for NK cell immune evasion in childhood B-acute lymphoblastic leukemia. *Leukemia*. 2016;30(4):800-811.
26. Schwartz S, Rieder H, Schlager B, Burmeister T, Fischer L, Thiel E. Expression of the human homologue of rat NG2 in adult acute lymphoblastic leukemia: close association with MLL rearrangement and a CD10(-)/CD24(-)/CD65s(+)/CD15(+) B-cell phenotype. *Leukemia*. 2003;17(8):1589-1595.
27. Bardini M, Woll PS, Corral L, et al. Clonal variegation and dynamic competition of leukemia-initiating cells in infant acute lymphoblastic leukemia with MLL rearrangement. *Leukemia*. 2015;29(1):38-50.
28. Popovic R, Riesbeck LE, Velu CS, et al. Regulation of mir-196b by MLL and its overexpression by MLL fusions contributes to immortalization. *Blood*. 2009;113(14):3314-3322.
29. Lechman ER, Gentner B, van Galen P, et al. Attenuation of miR-126 activity expands HSC in vivo without exhaustion. *Cell stem cell*. 2012;11(6):799-811.
30. Godfrey L, Kerry J, Thorne R, et al. MLL-AF4 binds directly to a BCL-2 specific enhancer and modulates H3K27 acetylation. *Experimental Hematology*. 2017;47:64-75.
31. Thomas M, Geßner A, Vornlocher H-P, Hadwiger P, Greil J, Heidenreich O. Targeting *MLL-AF4* with short interfering RNAs inhibits clonogenicity and engraftment of t(4;11)-positive human leukemic cells. *Blood*. 2005;106(10):3559-3566.
32. Agraz-Doblas A, Bueno C, Bashford-Rogers R, et al. Unravelling the cellular origin and clinical prognostic markers of infant B-cell acute lymphoblastic leukemia using genome-wide analysis. *Haematologica*. 2019:haematol.2018.206375.
33. Lin S, Luo RT, Shrestha M, Thirman MJ, Mulloy JC. The full transforming capacity of MLL-Af4 is interlinked with lymphoid lineage commitment. *Blood*. 2017;130(7):903-907.
34. Sinclair PB, Blair HH, Ryan SL, et al. Dynamic clonal progression in xenografts of acute lymphoblastic leukemia with intrachromosomal amplification of chromosome 21. *Haematologica*. 2018;103(4):634-644.
35. Lu B, Klingbeil O, Tarumoto Y, et al. A Transcription Factor Addiction in Leukemia Imposed by the MLL Promoter Sequence. *Cancer Cell*. 2018;34(6):970-981.e978.
36. Babicki S, Arndt D, Marcu A, et al. Heatmapper: web-enabled heat mapping for all. *Nucleic Acids Research*. 2016;44(W1):W147-W153.
37. Wilkinson Adam C, Ballabio E, Geng H, et al. RUNX1 Is a Key Target in t(4;11) Leukemias that Contributes to Gene Activation through an AF4-MLL Complex Interaction. *Cell Reports*. 2013;3(1):116-127.
38. Muñoz-López A, Romero-Moya D, Prieto C, et al. Development Refractoriness of MLL-Rearranged Human B Cell Acute Leukemias to Reprogramming into Pluripotency. *Stem Cell Reports*. 2016;7(4):602-618.
39. Deshpande Aniruddha J, Deshpande A, Sinha Amit U, et al. AF10 Regulates Progressive H3K79 Methylation and HOX Gene Expression in Diverse AML Subtypes. *Cancer Cell*. 2014;26(6):896-908.
40. Mandal M, Hamel KM, Maienschein-Cline M, et al. Histone Reader BRWD1 Targets and Restricts Recombination to the Igk Locus. *Nature immunology*. 2015;16(10):1094-1103.
41. Smith L-L, Yeung J, Zeisig Bernd B, et al. Functional Crosstalk between Bmi1 and MLL/Hoxa9 Axis in Establishment of Normal Hematopoietic and Leukemic Stem Cells. *Cell Stem Cell*. 2011;8(6):649-662.
42. Yang Y, Chen Y, Saha MN, et al. Targeting phospho-MARCKS overcomes drug-resistance and induces antitumor activity in preclinical models of multiple myeloma. *Leukemia*. 2014;29(3):715-726.

43. Liu H, Westergard TD, Cashen A, et al. Proteasome Inhibitors Evoke Latent Tumor Suppression Programs in Pro-B MLL Leukemias Through MLL-AF4. *Cancer cell*. 2014;25(4):530-542.
44. Hirabayashi S, Ohki K, Nakabayashi K, et al. ZNF384-related fusion genes define a subgroup of childhood B-cell precursor acute lymphoblastic leukemia with a characteristic immunotype. *Haematologica*. 2017;102(1):118-129.
45. Agarwal V, Bell GW, Nam J-W, Bartel DP. Predicting effective microRNA target sites in mammalian mRNAs. *eLife*. 2015;4:e05005.
46. Krek A, Grün D, Poy MN, et al. Combinatorial microRNA target predictions. *Nature Genetics*. 2005;37(5):495-500.
47. Ding T, Li Z, Hailemariam T, et al. SMS overexpression and knockdown: impact on cellular sphingomyelin and diacylglycerol metabolism, and cell apoptosis. *Journal of Lipid Research*. 2008;49(2):376-385.
48. Mi S, Lu J, Sun M, et al. MicroRNA expression signatures accurately discriminate acute lymphoblastic leukemia from acute myeloid leukemia. *Proceedings of the National Academy of Sciences*. 2007;104(50):19971- 19976.
49. Pui CH, Frankel LS, Carroll AJ, et al. Clinical characteristics and treatment outcome of childhood acute lymphoblastic leukemia with the t(4;11)(q21;q23): a collaborative study of 40 cases. *Blood*. 1991;77(3):440-447.
50. Carulli G, Marini A, Ferreri MI, et al. B-cell acute lymphoblastic leukemia with t(4;11)(q21;q23) in a young woman: evolution into mixed phenotype acute leukemia with additional chromosomal aberrations in the course of therapy. *Hematology Reports*. 2012;4(3):e15.
51. Stass S, Mirro J, Melvin S, Pui CH, Murphy SB, Williams D. Lineage switch in acute leukemia. *Blood*. 1984;64(3):701-706.
52. Gardner R, Wu D, Cherian S, et al. Acquisition of a CD19-negative myeloid phenotype allows immune escape of MLL-rearranged B-ALL from CD19 CAR-T-cell therapy. *Blood*. 2016;127(20):2406-2410.
53. Jacoby E, Nguyen SM, Fountaine TJ, et al. CD19 CAR immune pressure induces B-precursor acute lymphoblastic leukaemia lineage switch exposing inherent leukaemic plasticity. *Nature Communications*. 2016;7(1):12320.
54. McClellan JS, Majeti R. The cancer stem cell model: B cell acute lymphoblastic leukaemia breaks the mould. *EMBO Molecular Medicine*. 2013;5(1):7-9.

Figure legends.

Figure 1. MiR-130b and miR-128a are upregulated in patient blasts and have tumorigenic functions in MLL-AF4+ B-ALL cells

(A) Experimental approach and sorting strategy of bone marrow cells from patients. (B) Differential expression analysis of microRNAs in blasts at diagnosis (CD19+CD10-NG2+CD34+, CD19+CD10-NG2-CD34+ and CD19+CD10-CD34-) versus non-blasts at remission (CD19-CD10-). Data were compared using a limma test. Expression of (C) miR-130b and (D) miR-128a in patients' leukemic blasts (diagnosis), non-blasts (remission) and human FL hematopoietic cells (10-20 wpc). (E) ATAC-Seq profiles of human FL LMPP derived from 10-20 wpc (n=2) and SEM cells (GSE117865) alongside FLAG-MLL-Af4 ChIP-Seq profiles of miR-130b and miR-128a loci in MLL-Af4 human leukemic blasts (GSE84116). The grey box highlights the promoter that regulate each microRNA. Arrows indicate an open chromatin region or a chromatin region with MLL-AF4 binding. Expression of *MLL-AF4*, *MEIS1*, *HOXA9*, *CDK6*, *BCL2*, miR-130b and miR-128a in SEM cells transfected with siRNA against MLL-AF4 (siMA6) after (F) 48h and (G) 72h. The log2-fold change (LOG2FC) is calculated using SEM sicontrol as a reference. (H) Proliferation after 72h in culture (initial cells concentration: 10^5 cells/mL) and (I) apoptosis assay in SEM cells when the activity of miR-130b and/or miR-128a is inhibited (pmiRZip-130b/128a). pmiRZip-scramble was used as a control. (J) Survival curve of SEM pmiRZip-scramble-, pmiRZip-130b- and pmiRZip-128a-engrafted NSG recipients. MicroRNA inhibition in leukemic cells was achieved through lentiviral transduction and monitored with GFP. Unless stated otherwise, data were compared using a Mann-Whitney U test: $p < 0.05$ (*), $p < 0.01$ (**), $p < 0.001$ (***), $p < 0.0001$ (****). Experiments were conducted in triplicate or more. Graphs are presented as Mean ± SEM.

Figure 2. MiR-130b and miR-128a promote the B-lymphoid bias of fetal liver Mll-AF4+ pre-leukemic cells

(A) Expression of miR-130b and miR-128a in E14 FL HSC/MPP and LMPP from Mll-AF4- VEC-Cre+ and Mll-AF4+ VEC-Cre+ embryos. (B) ATAC-Seq of mouse E14.5 FL LMPP (WT and Mll-AF4+ VEC-Cre+). Each trace represents a pool of 4 biological

replicates. The grey box highlights the promoter that regulate each microRNA. Arrows indicate an open chromatin region. (C) Expression of miR-130b or (D) miR-128a in transduced FL Mll-AF4+ LSK. (E) Experimental approach for the lentiviral transduction of FL Mll-AF4+ LSK and functional validation. Transduced cells were monitored with GFP expression. Clonogenic potential of transduced LSK in (F) myeloid and (G) B-lymphoid conditions. (H) Proliferation of myeloid and lymphoid cells in colony-forming assays. Data were compared using a Mann-Whitney U test: $p < 0.05$ (*), $p < 0.01$ (**), $p < 0.001$ (***), $p < 0.0001$ (****). Experiments were conducted in triplicate or more. Graphs are presented as Mean ± SEM.

Figure 3. The overexpression of miR-130b and miR-128a in Mll-AF4+ FL LSK leads to a mixed/BCP/myeloid or lymphoblastic acute leukemia, respectively

(A) Experimental design. All mice received Mll-AF4-expressing cells. Survival curve of primary, secondary and tertiary recipients of the (B) Mll-AF4+ pMIRH-130b and (C) Mll-AF4+ pMIRH-128a cohorts. Total bone marrow from 1-2 primary recipients were used for secondary transplants. Total bone marrow from 2-3 recipients were used for tertiary transplants. Positive event = hematological malignancy linked to donor cells. A Gehan-Breslow-Wilcoxon test was used to compare survival curves. (D) Types of malignancies in Mll-AF4+ control, Mll-AF4+ pMIRH-130b and Mll-AF4+ pMIRH-128a primary recipients. A Chi-square test was used to compare the distribution of sick and non-sick mice. (E) Post-mortem pictures of sick mice from the Mll-AF4+ control, Mll-AF4+ pMIRH-130b and Mll-AF4+ pMIRH-128a cohorts. (F) Spleen and (G) liver weights. (H) GFP chimerism in the bone marrow. (I) White blood cell counts in Mll-AF4+ control and sick mice. Proportion of (J) myeloid cells, (K) mixed lineage cells, (L) B-lymphoid cells, (M) ckit+ cells and (N) IgM+ and Il7r+ cells in the GFP+ fraction of the bone marrow of Mll-AF4+ control and sick mice (Mll-AF4+ pMIRH-130b or Mll-AF4+ pMIRH-128a). (O) Proportion of LSK Il7r+Flt3-, HSC/MPP (LSK Il7r- Flt3-) and LMPP (LSK Flt3+) in the LSK compartment of control and sick mice. (P) Central nervous system infiltration in Mll-AF4+ control, Mll-AF4+ pMIRH-130b and Mll-AF4+ pMIRH-128a mice. The level of infiltration is described in the material and methods section. (Q) Romanowsky staining of peripheral blood smears. All images are at the same magnification according to the scale. Data were compared using a Mann-Whitney U test: $p < 0.05$ (*), $p < 0.01$ (**), $p < 0.001$ (***), $p < 0.0001$ (****). Graphs are presented as Mean ± SEM (one dot = one mouse).

Figure 4. Mll-AF4+ pMIRH-130b/pMIRH-128a+ cells display a gene expression profile similar to MLL-AF4+ patient blasts

(A) *Mll-AF4* expression in transduced/GFP+ E14 FL Mll-AF4+ LSK (pre-leukemia and pre-transplantation). (B) Heatmap of gene expression in transduced E14 FL Mll-AF4+ LSK. (C) Summary of the gene expression results of transduced E14 FL Mll-AF4+ LSK. (D) *Mll-AF4* expression in total bone marrow cells of control and leukemic mice. (E) Heatmap of gene expression in total bone marrow cells. (F) Summary of the gene expression results of total bone marrow cells. Data were compared using a Mann-Whitney U test: $p < 0.05$ (*), $p < 0.01$ (**), $p < 0.001$ (***), $p < 0.0001$ (****). Experiments were conducted in triplicate or more. Heatmaps present the log2-fold change (log2FC) of gene expression, using Mll-AF4+ pMIRH (Control) as a reference.

Figure 5. Mll-AF4+ pMIRH-130b and Mll-AF4+ pMIRH-128a leukemia are propagated by different LSCs

(A) Experimental design. All sorted cells were retrieved from recipients originally transplanted with total bone marrow cells. Secondary recipients received cells retrieved from the bone marrow of FL Mll-AF4+ LSK primary recipients. Tertiary recipients received cells from the bone marrow of total bone marrow secondary recipients. Survival curves of (B) secondary and (C) tertiary transplants of mice that received sorted HSC/MPP (LSK Il7r- Flt3-), LMPP (LSK Flt3+) or LK/CLP (Lineage-Sca1low/-ckit+) from the bone marrow of Mll-AF4+ pMIRH-130b sick mice. Survival curves of (D) secondary and (E) tertiary transplants of mice that received sorted HSC/MPP, LMPP, LK/CLP or LSK Il7r+ from the bone marrow of Mll-AF4+ pMIRH-128a sick mice. GFP chimerism in the bone marrow of (F) secondary and (G) tertiary recipients. (H) Proportion of hematopoietic cells in secondary recipients of LMPP from Mll-AF4+ pMIRH-130b sick mice. Spleen and liver weight are also indicated. (I) Spleen and (J) liver weight of sick tertiary recipients that received sorted HSC/MPP, LMPP, LK/CLP or LSK Il7r+ from the bone marrow of Mll-AF4+ pMIRH-130b or Mll-AF4+ pMIRH-128a sick mice. (K) Proportion of myeloid cells, mixed lineage cells, B-lymphoid cells and ckit+ Il7r+ cells. (L) T-lymphoid cells in the bone marrow of tertiary recipients of sorted cells from Mll-AF4+ pMIRH-130b or Mll-AF4+ pMIRH-128a sick mice. Proportion of (M) ckit+ cells and (N) HSC/MPP, LMPP and LSK Il7r+

cells in the bone marrow LSK compartment of tertiary recipients of sorted cells from Mll-AF4+ pMIRH-130b sick mice. Graphs are presented as Mean ± SEM (one dot = one mouse).

Figure 6. NR2F6 and SGMS1, two targets of miR-130b and miR-128a, have tumor suppressive activity in MLL-AF4-driven leukemogenesis

(A) Overlap of deregulated genes in GSE79533 and GSE79450 data sets (black), predicted targets of miR-130b (green) or miR-128a (blue) using TargetScan and PicTar. (B) *NR2F6* and (C) *SGMS1* expression in t(4;11) MLL-AF4 pediatric leukemia blasts and non-blasts from our cohort. (D) *Nr2f6* and (E) *Sgms1* expression in FL Mll-AF4+ LSK (pre-leukemic) and bone marrow (leukemic) of Mll-AF4+ pMIRH control mice and of Mll-AF4+ pMIRH-130b and Mll-AF4+ pMIRH-128a sick mice. (F) RT-qPCR of miR-130b, miR-128a, *MLL-AF4*, *MEIS1*, *HOXA9*, *CDK6*, *BCL2*, *NR2F6* and *SGMS1* in SEM cells transfected with a negative inhibitor control, miR-130b inhibitor or miR-128a inhibitor. The log2-fold change (LOG2FC) is calculated using the negative inhibitor control as a reference. (G) Western blot against NR2F6 and SGMS1 in SEM cells transfected with a negative inhibitor control, miR-130b inhibitor or miR-128a inhibitor. The brightness was adjusted manually in ImageJ to uniform the background, and each lane came from the same membrane. The WT lane was not directly next to the siRNAs lane and is separated by a vertical line. Relative quantification for all three proteins was calculated by Image Lab using the sicontrol as a reference. The quantification presented for NR2F6 and SGMS1 is adjusted with the relative quantification of the β-actin signal intensity. The β-actin signal comes from the same membrane as the NR2F6/SGMS1 signal (n=4). (H) Apoptosis and (I) proliferation of SEM leukemic cells upon NR2F6 and SGMS1 overexpression. (J) Expression of *MLL-AF4* and its target genes (*MEIS1*, *HOXA9*, *CDK6*, *BCL2,* miR-130b and miR-128a) and *SGMS1* in SEM leukemic cells upon NR2F6 overexpression. The log2-fold change (LOG2FC) is calculated using SEM pCDH cells as a reference. (K) Survival curve of NSG mice transplanted with SEM control (pCDH-empty) and overexpressing NR2F6 (pCDH-NR2F6). NSG mice were culled 64 days after transplant due to facility concerns. This experiment could not be performed with SGMS1 due to the high amount of cell death in SEM cells. The overexpression of NR2F6 and SGMS1 in leukemic cells was achieved by lentiviral transduction and transduced cells were monitored with GFP. A Gehan-Breslow-Wilcoxon test was used to compare survival curves. Unless stated otherwise, data

were compared using a Mann-Whitney U test: $p < 0.05$ (*), $p < 0.01$ (**), $p < 0.001$ (***), $p < 0.0001$ (****). Graphs are presented as Mean ± SEM.

Figure 7. Continued miR-130b activity and NR2F6/SGMS1 inhibition is required for MLL-AF4+ leukemia maintenance

(A) Experimental layout of rescue experiment for Mll-AF4+ pMIRH-130b leukemic mice (18 000 GFP+ cells injected) and Mll-AF4+ pMIRH-128a leukemic mice (10 000 GFP+ cells injected). (B) Survival curve of Mll-AF4+ pMIRH-130b rescue mice (pmiRZip-scramble or pmiRZip-130b, NR2F6 of SGMS1 overexpression). (C) GFP chimerism in various organs of Mll-AF4+ pMIRH-130b rescue mice. (D) Lineage output in the GFP+ fraction of the bone marrow of Mll-AF4+ pMIRH-130b rescue mice. (E) Survival curve of Mll-AF4+ pMIRH-128a rescue mice with microRNA inhibition (pmiRZip-scramble, pmiRZip-128a, pmiRZip-130b or pmiRZip-128a+130b). (F) Survival curve of Mll-AF4+ pMIRH-128a rescue mice with NR2F6 or SGMS1 overexpression. A statistical comparison of the survival rate of rescue mice was performed using a Chi-square test to compare the distribution of sick and non-sick mice (indicated next to the number of sick mice/total mice). (G) GFP chimerism in the bone marrow of Mll-AF4+ pMIRH-128a rescue mice. (H) Post-mortem photos of representative Mll-AF4+ pMIRH-128a rescue mice. (I) Apoptosis/necrosis of fresh GFP+ cells retrieved from the bone marrow of Mll-AF4+ pMIRH-130b and Mll-AF4+ pMIRH-128a rescue mice upon NR2F6 or SGMS1 overexpression. Recipients of SGMS1-overexpressing cells were sacrificed because of a stroke-like phenotype. Data were compared using a Mann-Whitney U test: $p < 0.05$ (*), $p < 0.01$ (**), $p < 0.001$ (***). A Gehan-Breslow-Wilcoxon test was used to compare survival curves. Graphs are presented as Mean ± SEM (one dot = one mouse).

Figure 1

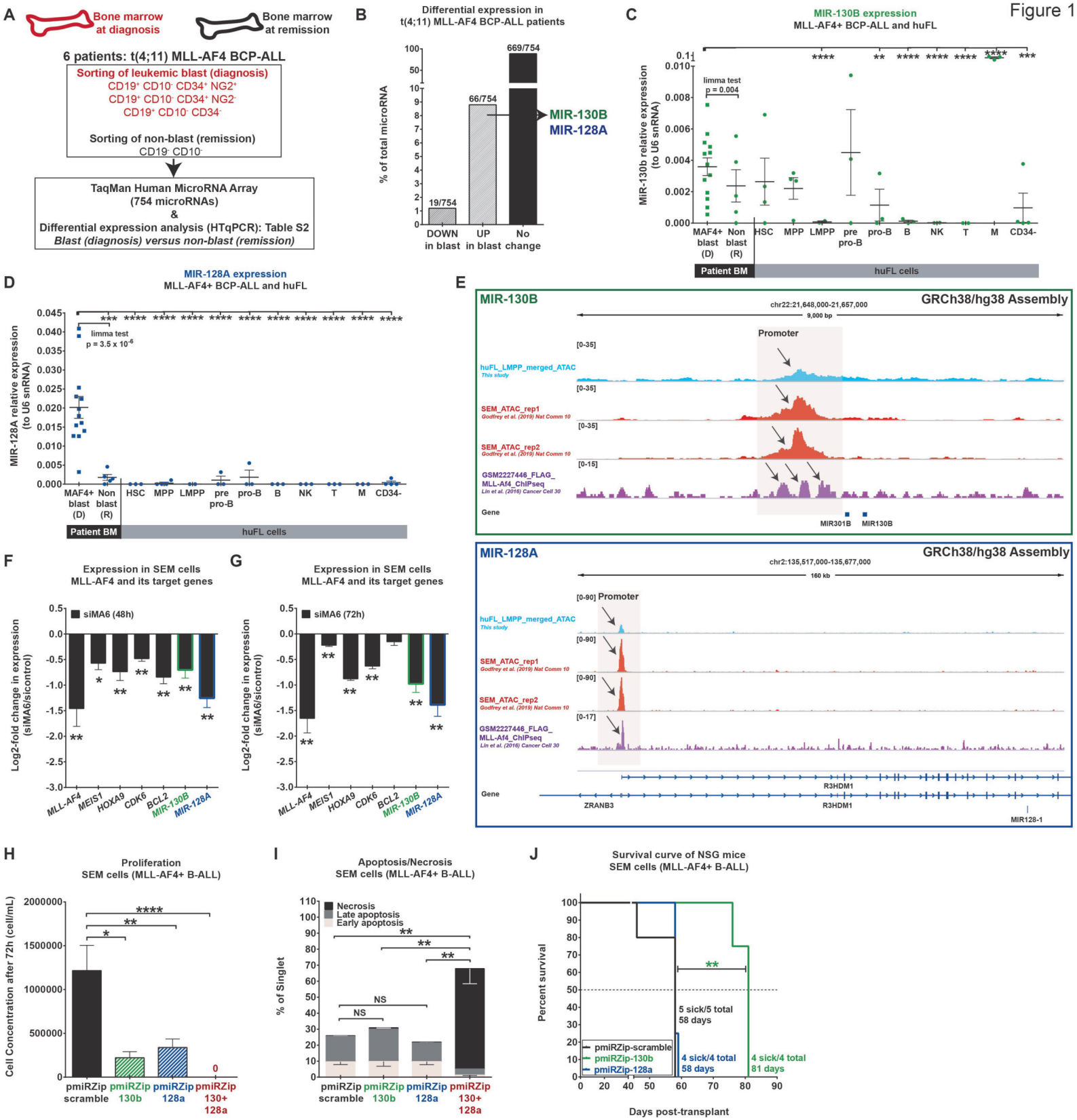
A
Bone marrow at diagnosis
Bone marrow at remission
6 patients: t(4;11) MLL-AF4 BCP-ALL
Sorting of leukemic blast (diagnosis)
CD19+ CD10- CD34+ NG2+
CD19+ CD10- CD34+ NG2-
CD19+ CD10- CD34-
Sorting of non-blast (remission)
CD19- CD10-
TaqMan Human MicroRNA Array
(754 microRNAs)
&
Differential expression analysis (HTqPCR): Table S2
Blast (diagnosis) versus non-blast (remission)
B
Differential expression in
t(4;11) MLL-AF4 BCP-ALL patients
% of total microRNA
669/754
66/754
19/754
MIR-130B
MIR-128A
DOWN in blast
UP in blast
No change
C
MIR-130B expression
MLL-AF4+ BCP-ALL and huFL
MiR-130b relative expression (to U6 snRNA)
limma test p = 0.004
MAF4+ blast (D)
Non blast (R)
HSC
MPP
LMPP
pre pro-B
pro-B
B
NK
T
M
CD34-
Patient BM
huFL cells
D
MIR-128A expression
MLL-AF4+ BCP-ALL and huFL
MIR-128A relative expression (to U6 snRNA)
limma test p = 3.5 x 10-6
E
MIR-130B
GRCh38/hg38 Assembly
chr22:21,648,000-21,657,000
9,000 bp
Promoter
huFL_LMPP_merged_ATAC
This study
SEM_ATAC_rep1
Godfrey et al. (2019) Nat Comm 10
SEM_ATAC_rep2
GSM2227446_FLAG_MLL-Af4_ChIPseq
Lin et al. (2016) Cancer Cell 30
Gene
MIR301B
MIR130B
MIR-128A
GRCh38/hg38 Assembly
chr2:135,517,000-135,677,000
160 kb
R3HDM1
ZRANB3
MIR128-1
F
Expression in SEM cells
MLL-AF4 and its target genes
siMA6 (48h)
Log2-fold change in expression (siMA6/sicontrol)
MLL-AF4
MEIS1
HOXA9
CDK6
BCL2
MIR-130B
MIR-128A
G
Expression in SEM cells
MLL-AF4 and its target genes
siMA6 (72h)
H
Proliferation
SEM cells (MLL-AF4+ B-ALL)
Cell Concentration after 72h (cell/mL)
pmiRZip scramble
pmiRZip 130b
pmiRZip 128a
pmiRZip 130+ 128a
I
Apoptosis/Necrosis
SEM cells (MLL-AF4+ B-ALL)
Necrosis
Late apoptosis
Early apoptosis
% of Singlet
NS
J
Survival curve of NSG mice
SEM cells (MLL-AF4+ B-ALL)
Percent survival
5 sick/5 total
58 days
pmiRZip-scramble
pmiRZip-130b
pmiRZip-128a
4 sick/4 total
58 days
4 sick/4 total
81 days
Days post-transplant

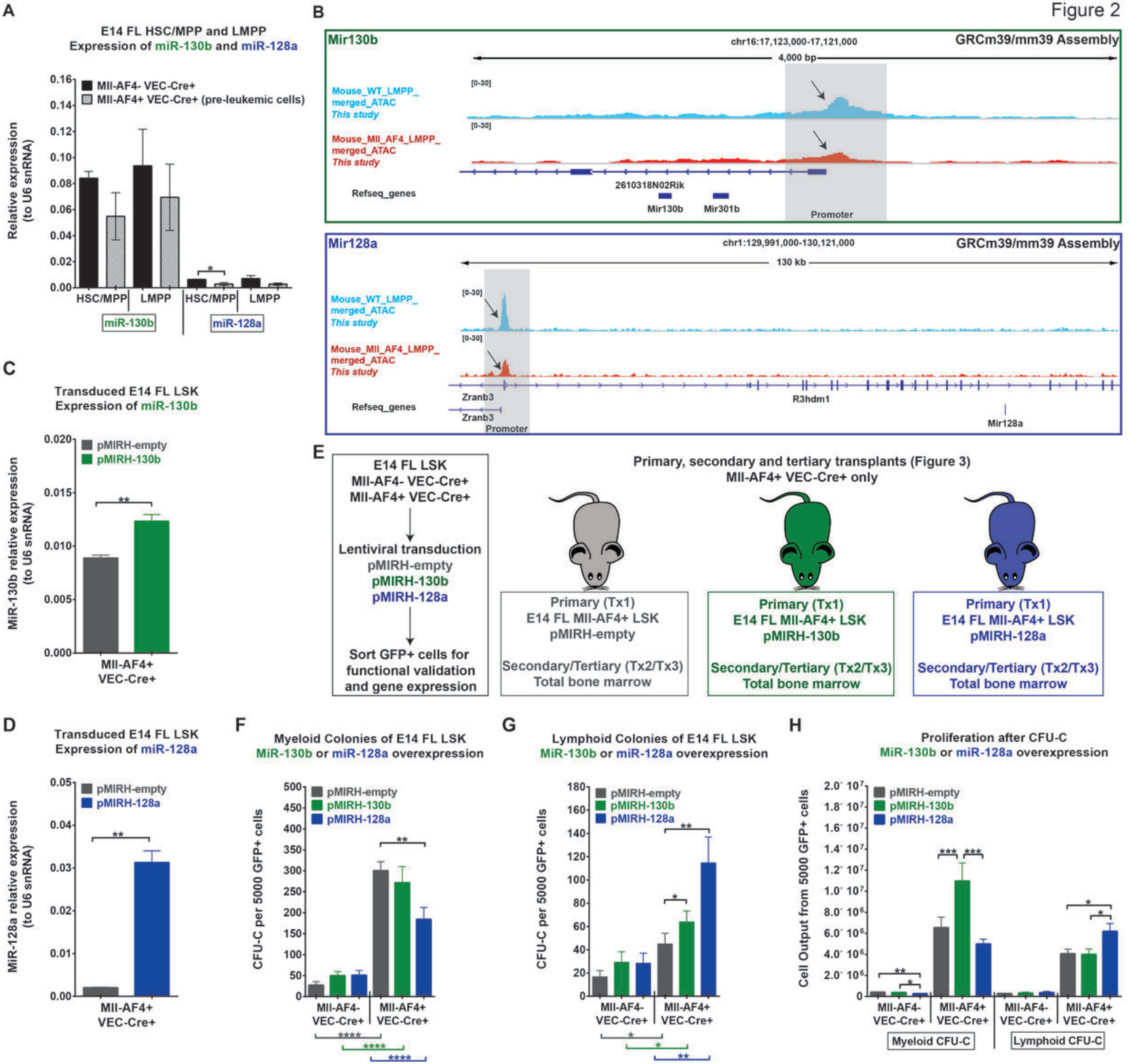
A
E14 FL HSC/MPP and LMPP
Expression of miR-130b and miR-128a
Mll-AF4- VEC-Cre+
Mll-AF4+ VEC-Cre+ (pre-leukemic cells)
Relative expression (to U6 snRNA)
HSC/MPP
LMPP
HSC/MPP
LMPP
miR-130b
miR-128a
B
Mir130b
chr16:17,123,000-17,121,000
GRCm39/mm39 Assembly
4,000 bp
Mouse_WT_LMPP_ merged_ATAC This study
Mouse_Mll_AF4_LMPP_ merged_ATAC This study
Refseq_genes
2610318N02Rik
Mir130b
Mir301b
Promoter
Mir128a
chr1:129,991,000-130,121,000
GRCm39/mm39 Assembly
130 kb
Zranb3
R3hdm1
Mir128a
C
Transduced E14 FL LSK
Expression of miR-130b
pMIRH-empty
pMIRH-130b
MiR-130b relative expression (to U6 snRNA)
Mll-AF4+ VEC-Cre+
D
Transduced E14 FL LSK
Expression of miR-128a
pMIRH-empty
pMIRH-128a
MiR-128a relative expression (to U6 snRNA)
Mll-AF4+ VEC-Cre+
E
E14 FL LSK
Mll-AF4- VEC-Cre+
Mll-AF4+ VEC-Cre+
Lentiviral transduction
pMIRH-empty
pMIRH-130b
pMIRH-128a
Sort GFP+ cells for functional validation and gene expression
Primary, secondary and tertiary transplants (Figure 3)
Mll-AF4+ VEC-Cre+ only
Primary (Tx1)
E14 FL Mll-AF4+ LSK
pMIRH-empty
Secondary/Tertiary (Tx2/Tx3)
Total bone marrow
Primary (Tx1)
E14 FL Mll-AF4+ LSK
pMIRH-130b
Secondary/Tertiary (Tx2/Tx3)
Total bone marrow
Primary (Tx1)
E14 FL Mll-AF4+ LSK
pMIRH-128a
Secondary/Tertiary (Tx2/Tx3)
Total bone marrow
F
Myeloid Colonies of E14 FL LSK
MiR-130b or miR-128a overexpression
CFU-C per 5000 GFP+ cells
pMIRH-empty
pMIRH-130b
pMIRH-128a
Mll-AF4- VEC-Cre+
Mll-AF4+ VEC-Cre+
G
Lymphoid Colonies of E14 FL LSK
MiR-130b or miR-128a overexpression
CFU-C per 5000 GFP+ cells
pMIRH-empty
pMIRH-130b
pMIRH-128a
Mll-AF4- VEC-Cre+
Mll-AF4+ VEC-Cre+
H
Proliferation after CFU-C
MiR-130b or miR-128a overexpression
Cell Output from 5000 GFP+ cells
pMIRH-empty
pMIRH-130b
pMIRH-128a
Mll-AF4- VEC-Cre+
Mll-AF4+ VEC-Cre+
Mll-AF4- VEC-Cre+
Mll-AF4+ VEC-Cre+
Myeloid CFU-C
Lymphoid CFU-C

Figure 3

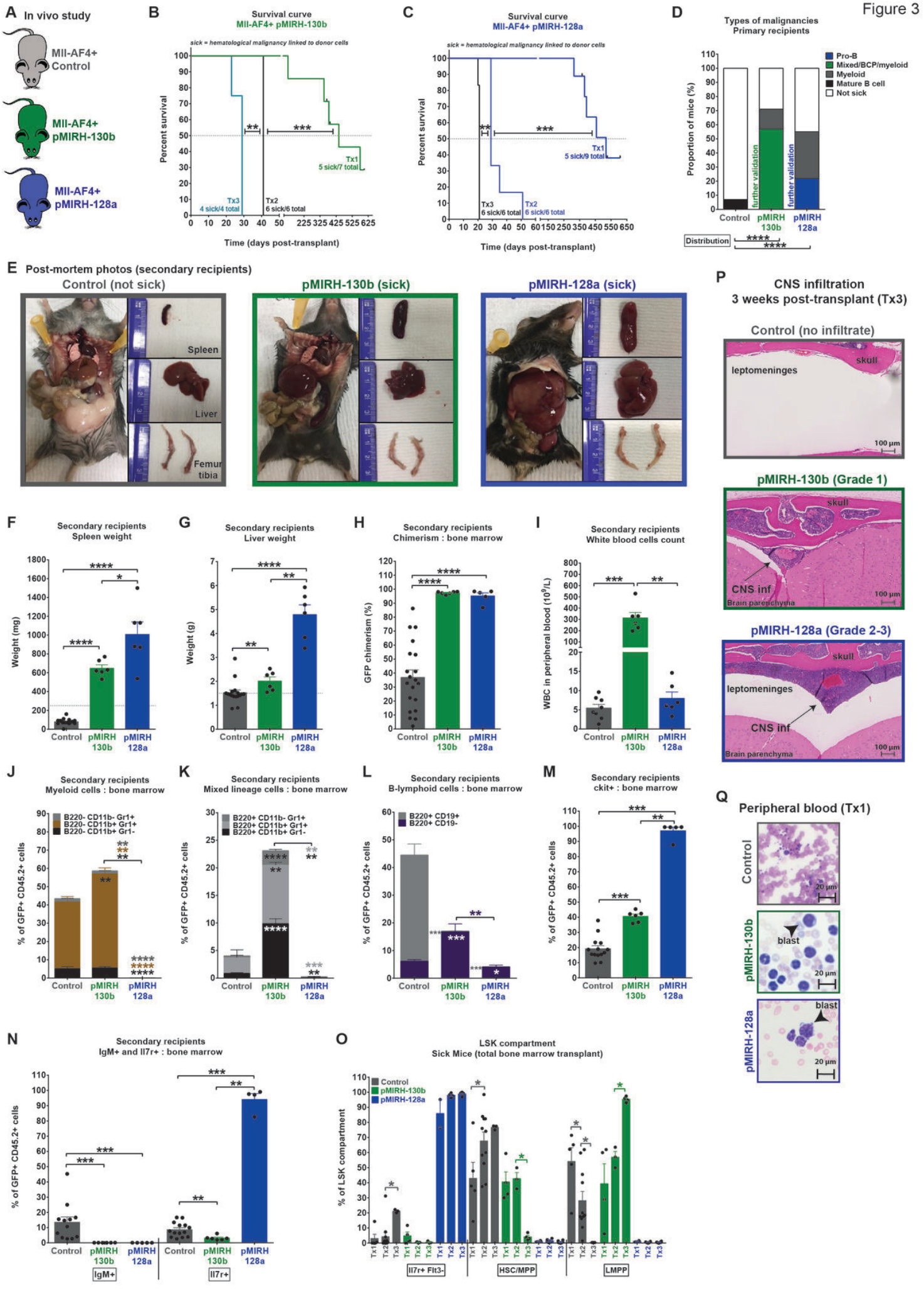
A In vivo study
MII-AF4+ Control
MII-AF4+ pMIRH-130b
MII-AF4+ pMIRH-128a
B Survival curve MII-AF4+ pMIRH-130b
sick = hematological malignancy linked to donor cells
Percent survival
Time (days post-transplant)
Tx3 4 sick/4 total
Tx2 6 sick/6 total
Tx1 5 sick/7 total
C Survival curve MII-AF4+ pMIRH-128a
Tx3 6 sick/6 total
Tx2 6 sick/6 total
Tx1 5 sick/9 total
D Types of malignancies Primary recipients
Proportion of mice (%)
Pro-B
Mixed/BCP/myeloid
Myeloid
Mature B cell
Not sick
further validation
Control
pMIRH 130b
pMIRH 128a
Distribution
E Post-mortem photos (secondary recipients)
Control (not sick)
pMIRH-130b (sick)
pMIRH-128a (sick)
Spleen
Liver
Femur
tibia
F Secondary recipients Spleen weight
Weight (mg)
G Secondary recipients Liver weight
Weight (g)
H Secondary recipients Chimerism : bone marrow
GFP chimerism (%)
I Secondary recipients White blood cells count
WBC in peripheral blood (10⁹/L)
J Secondary recipients Myeloid cells : bone marrow
B220- CD11b- Gr1+
B220- CD11b+ Gr1+
B220- CD11b+ Gr1-
% of GFP+ CD45.2+ cells
K Secondary recipients Mixed lineage cells : bone marrow
B220+ CD11b- Gr1+
B220+ CD11b+ Gr1+
B220+ CD11b+ Gr1-
L Secondary recipients B-lymphoid cells : bone marrow
B220+ CD19+
B220- CD19-
M Secondary recipients ckit+ : bone marrow
N Secondary recipients IgM+ and Il7r+ : bone marrow
IgM+
Il7r+
O LSK compartment Sick Mice (total bone marrow transplant)
Control
pMIRH-130b
pMIRH-128a
% of LSK compartment
Il7r+ Flt3-
HSC/MPP
LMPP
P CNS infiltration 3 weeks post-transplant (Tx3)
Control (no infiltrate)
leptomeninges
skull
100 µm
pMIRH-130b (Grade 1)
CNS inf
Brain parenchyma
pMIRH-128a (Grade 2-3)
Q Peripheral blood (Tx1)
Control
pMIRH-130b
pMIRH-128a
blast
20 µm

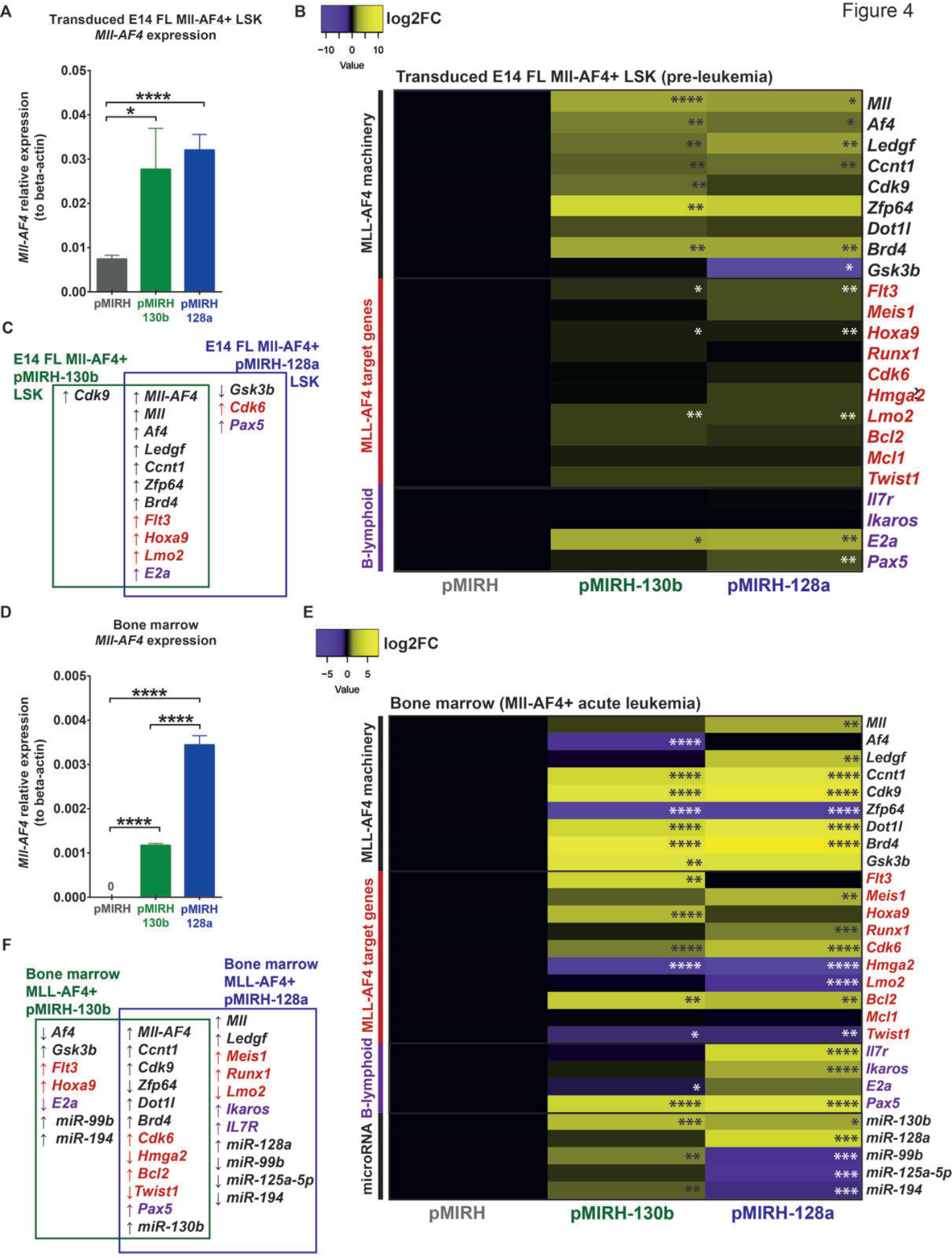
A
Transduced E14 FL Mll-AF4+ LSK
Mll-AF4 expression
Mll-AF4 relative expression (to beta-actin)
0.05
0.04
0.03
0.02
0.01
0.00
****
*
pMIRH
pMIRH 130b
pMIRH 128a
B
log2FC
−10 0 10
Value
Transduced E14 FL Mll-AF4+ LSK (pre-leukemia)
MLL-AF4 machinery
MLL-AF4 target genes
B-lymphoid
Mll
Af4
Ledgf
Ccnt1
Cdk9
Zfp64
Dot1l
Brd4
Gsk3b
Flt3
Meis1
Hoxa9
Runx1
Cdk6
Hmga2
Lmo2
Bcl2
Mcl1
Twist1
Il7r
Ikaros
E2a
Pax5
pMIRH
pMIRH-130b
pMIRH-128a
C
E14 FL Mll-AF4+ pMIRH-130b LSK
E14 FL Mll-AF4+ pMIRH-128a LSK
↑ Cdk9
↑ Mll-AF4
↑ Mll
↑ Af4
↑ Ledgf
↑ Ccnt1
↑ Zfp64
↑ Brd4
↑ Flt3
↑ Hoxa9
↑ Lmo2
↑ E2a
↓ Gsk3b
↑ Cdk6
↑ Pax5
D
Bone marrow
Mll-AF4 expression
Mll-AF4 relative expression (to beta-actin)
0.005
0.004
0.003
0.002
0.001
0.000
****
****
****
0
pMIRH
pMIRH 130b
pMIRH 128a
E
log2FC
−5 0 5
Value
Bone marrow (Mll-AF4+ acute leukemia)
MLL-AF4 machinery
MLL-AF4 target genes
B-lymphoid
microRNA
Mll
Af4
Ledgf
Ccnt1
Cdk9
Zfp64
Dot1l
Brd4
Gsk3b
Flt3
Meis1
Hoxa9
Runx1
Cdk6
Hmga2
Lmo2
Bcl2
Mcl1
Twist1
Il7r
Ikaros
E2a
Pax5
miR-130b
miR-128a
miR-99b
miR-125a-5p
miR-194
pMIRH
pMIRH-130b
pMIRH-128a
F
Bone marrow MLL-AF4+ pMIRH-130b
↓ Af4
↑ Gsk3b
↑ Flt3
↑ Hoxa9
↓ E2a
↑ miR-99b
↑ miR-194
↑ Mll-AF4
↑ Ccnt1
↑ Cdk9
↓ Zfp64
↑ Dot1l
↑ Brd4
↑ Cdk6
↓ Hmga2
↑ Bcl2
↓ Twist1
↑ Pax5
↑ miR-130b
Bone marrow MLL-AF4+ pMIRH-128a
↑ Mll
↑ Ledgf
↑ Meis1
↑ Runx1
↓ Lmo2
↑ Ikaros
↑ IL7R
↑ miR-128a
↓ miR-99b
↓ miR-125a-5p
↓ miR-194

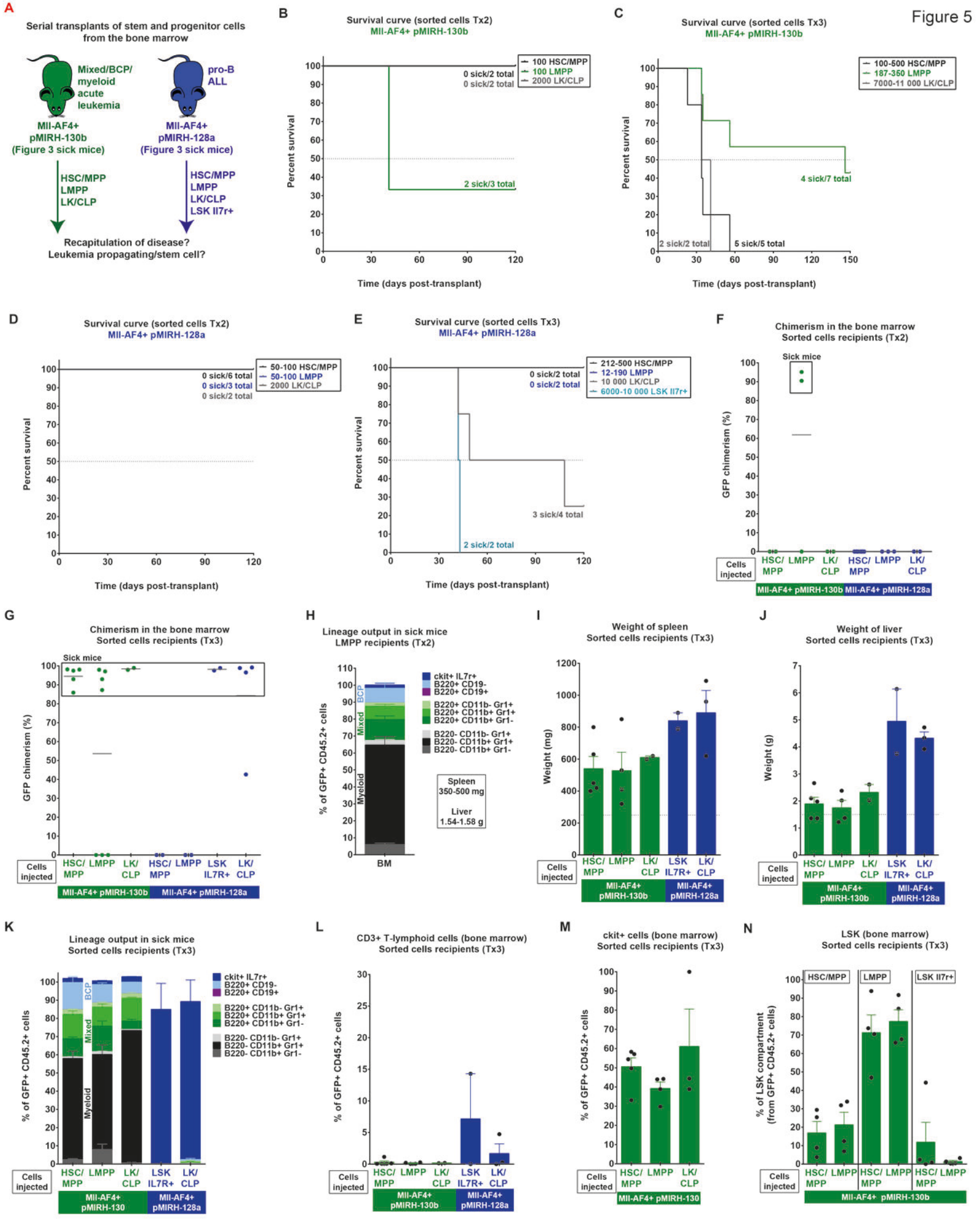
A
Serial transplants of stem and progenitor cells from the bone marrow
Mixed/BCP/ myeloid acute leukemia
pro-B ALL
MII-AF4+ pMIRH-130b (Figure 3 sick mice)
MII-AF4+ pMIRH-128a (Figure 3 sick mice)
HSC/MPP
LMPP
LK/CLP
HSC/MPP
LMPP
LK/CLP
LSK Il7r+
Recapitulation of disease?
Leukemia propagating/stem cell?
B
Survival curve (sorted cells Tx2)
MII-AF4+ pMIRH-130b
100 HSC/MPP
100 LMPP
2000 LK/CLP
0 sick/2 total
0 sick/2 total
2 sick/3 total
Percent survival
Time (days post-transplant)
C
Survival curve (sorted cells Tx3)
MII-AF4+ pMIRH-130b
100-500 HSC/MPP
187-350 LMPP
7000-11 000 LK/CLP
4 sick/7 total
2 sick/2 total
5 sick/5 total
Percent survival
Time (days post-transplant)
D
Survival curve (sorted cells Tx2)
MII-AF4+ pMIRH-128a
50-100 HSC/MPP
50-100 LMPP
2000 LK/CLP
0 sick/6 total
0 sick/3 total
0 sick/2 total
Percent survival
Time (days post-transplant)
E
Survival curve (sorted cells Tx3)
MII-AF4+ pMIRH-128a
212-500 HSC/MPP
12-190 LMPP
10 000 LK/CLP
6000-10 000 LSK Il7r+
0 sick/2 total
0 sick/2 total
3 sick/4 total
2 sick/2 total
Percent survival
Time (days post-transplant)
F
Chimerism in the bone marrow
Sorted cells recipients (Tx2)
Sick mice
GFP chimerism (%)
Cells injected
HSC/ MPP
LMPP
LK/ CLP
HSC/ MPP
LMPP
LK/ CLP
MII-AF4+ pMIRH-130b
MII-AF4+ pMIRH-128a
G
Chimerism in the bone marrow
Sorted cells recipients (Tx3)
Sick mice
GFP chimerism (%)
Cells injected
HSC/ MPP
LMPP
LK/ CLP
HSC/ MPP
LMPP
LSK IL7R+
LK/ CLP
MII-AF4+ pMIRH-130b
MII-AF4+ pMIRH-128a
H
Lineage output in sick mice
LMPP recipients (Tx2)
% of GFP+ CD45.2+ cells
BCP
Mixed
Myeloid
ckit+ IL7r+
B220+ CD19-
B220+ CD19+
B220+ CD11b- Gr1+
B220+ CD11b+ Gr1+
B220+ CD11b+ Gr1-
B220- CD11b- Gr1+
B220- CD11b+ Gr1+
B220- CD11b+ Gr1-
Spleen 350-500 mg
Liver 1.54-1.58 g
BM
I
Weight of spleen
Sorted cells recipients (Tx3)
Weight (mg)
Cells injected
HSC/ MPP
LMPP
LK/ CLP
LSK IL7R+
LK/ CLP
MII-AF4+ pMIRH-130b
MII-AF4+ pMIRH-128a
J
Weight of liver
Sorted cells recipients (Tx3)
Weight (g)
Cells injected
HSC/ MPP
LMPP
LK/ CLP
LSK IL7R+
LK/ CLP
MII-AF4+ pMIRH-130b
MII-AF4+ pMIRH-128a
K
Lineage output in sick mice
Sorted cells recipients (Tx3)
% of GFP+ CD45.2+ cells
BCP
Mixed
Myeloid
ckit+ IL7r+
B220+ CD19-
B220+ CD19+
B220+ CD11b- Gr1+
B220+ CD11b+ Gr1+
B220+ CD11b+ Gr1-
B220- CD11b- Gr1+
B220- CD11b+ Gr1+
B220- CD11b+ Gr1-
Cells injected
HSC/ MPP
LMPP
LK/ CLP
LSK IL7R+
LK/ CLP
MII-AF4+ pMIRH-130
MII-AF4+ pMIRH-128a
L
CD3+ T-lymphoid cells (bone marrow)
Sorted cells recipients (Tx3)
% of GFP+ CD45.2+ cells
Cells injected
HSC/ MPP
LMPP
LK/ CLP
LSK IL7R+
LK/ CLP
MII-AF4+ pMIRH-130b
MII-AF4+ pMIRH-128a
M
ckit+ cells (bone marrow)
Sorted cells recipients (Tx3)
% of GFP+ CD45.2+ cells
Cells injected
HSC/ MPP
LMPP
LK/ CLP
MII-AF4+ pMIRH-130
N
LSK (bone marrow)
Sorted cells recipients (Tx3)
HSC/MPP
LMPP
LSK Il7r+
% of LSK compartment (from GFP+ CD45.2+ cells)
Cells injected
HSC/ MPP
LMPP
HSC/ MPP
LMPP
HSC/ MPP
LMPP
MII-AF4+ pMIRH-130b

A

1. Differentially expressed in pediatric and infant t(4;11) MLL-AF4 ALL (2330 genes in common between GSE7933 and GSE79450)

2. Overlap with human predicted targets of miR-130b and miR-128a (TargetScan and PicTar)

3. Functional validation in FL MII-AF4+ LSK (pre-leukemia) and in SEM cells (leukemia)

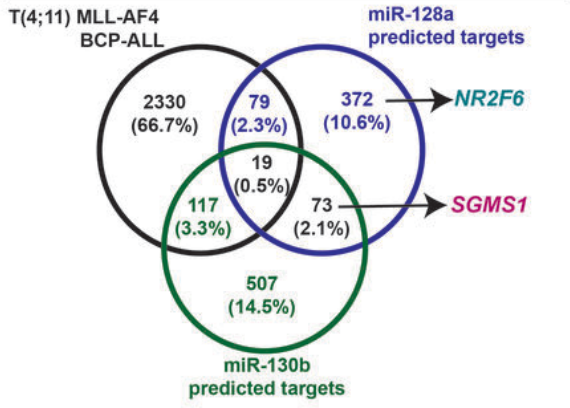

B

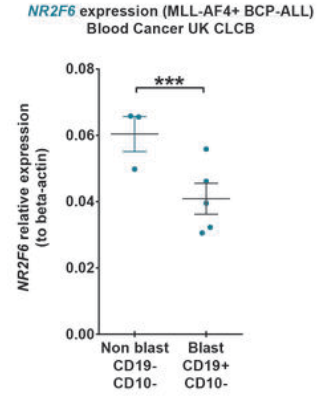

C

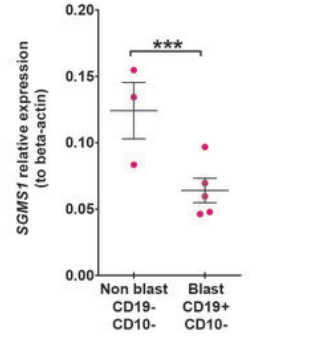

D

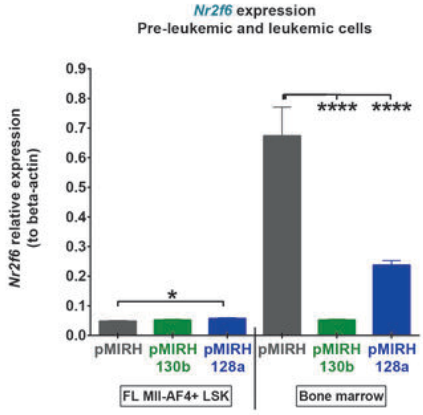

E

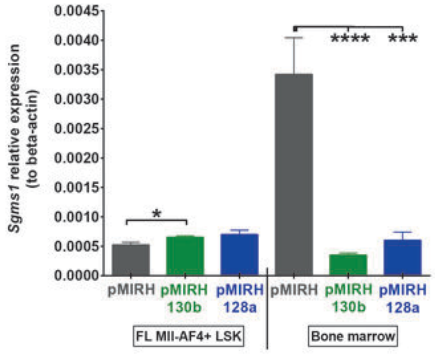

F

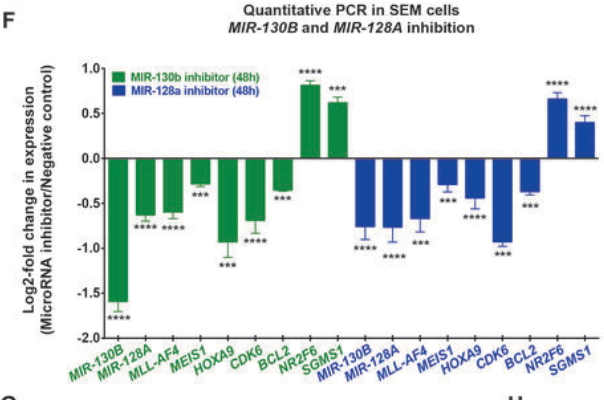

G

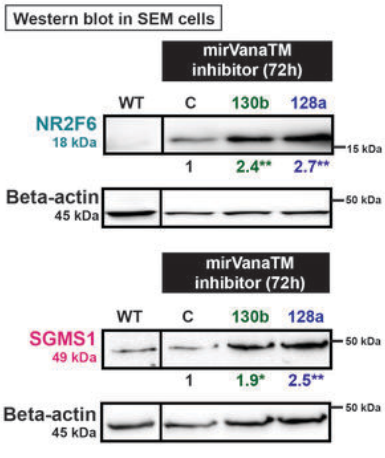

H

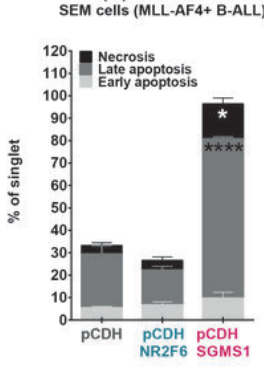

I

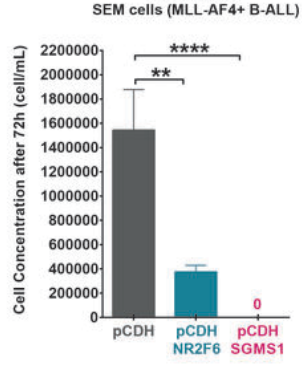

J

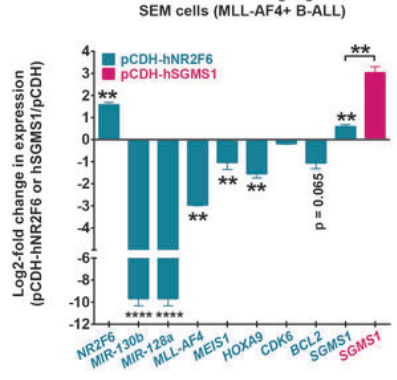

K

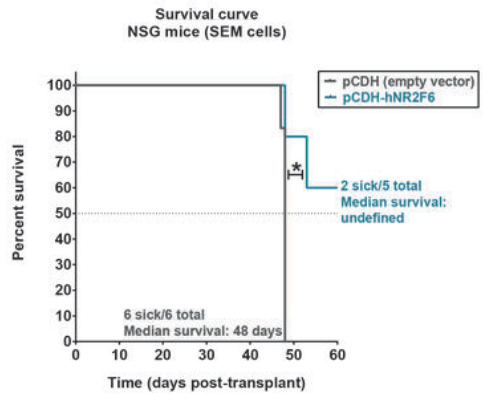

Figure 7

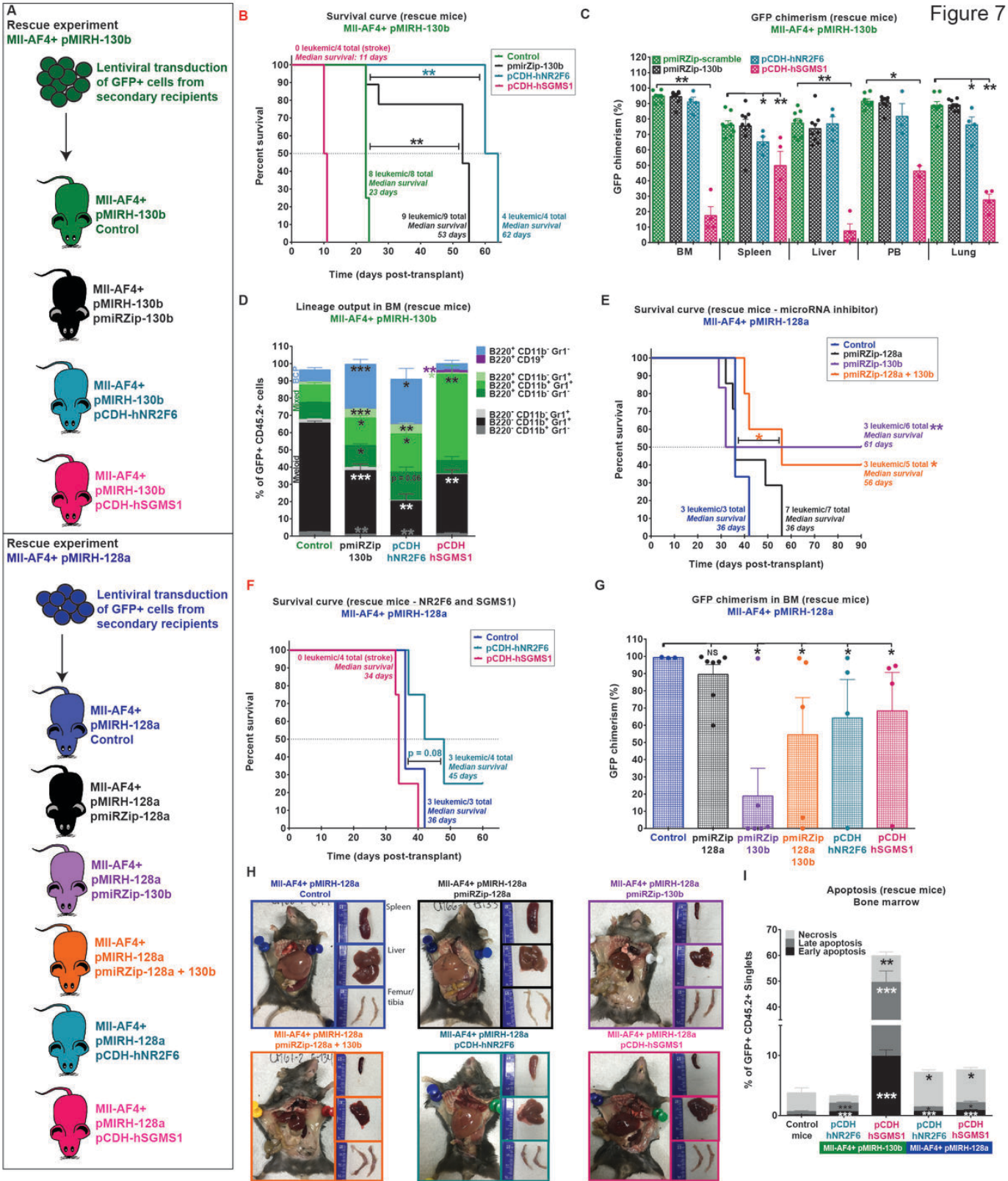
A
Rescue experiment
MII-AF4+ pMIRH-130b
Lentiviral transduction of GFP+ cells from secondary recipients
MII-AF4+ pMIRH-130b Control
MII-AF4+ pMIRH-130b pmiRZip-130b
MII-AF4+ pMIRH-130b pCDH-hNR2F6
MII-AF4+ pMIRH-130b pCDH-hSGMS1
Rescue experiment
MII-AF4+ pMIRH-128a
Lentiviral transduction of GFP+ cells from secondary recipients
MII-AF4+ pMIRH-128a Control
MII-AF4+ pMIRH-128a pmiRZip-128a
MII-AF4+ pMIRH-128a pmiRZip-130b
MII-AF4+ pMIRH-128a pmiRZip-128a + 130b
MII-AF4+ pMIRH-128a pCDH-hNR2F6
MII-AF4+ pMIRH-128a pCDH-hSGMS1
B
Survival curve (rescue mice)
MII-AF4+ pMIRH-130b
0 leukemic/4 total (stroke)
Median survival: 11 days
8 leukemic/8 total
Median survival
23 days
9 leukemic/9 total
Median survival
53 days
4 leukemic/4 total
Median survival
62 days
Control
pmiRZip-130b
pCDH-hNR2F6
pCDH-hSGMS1
Percent survival
Time (days post-transplant)
C
GFP chimerism (rescue mice)
MII-AF4+ pMIRH-130b
pmiRZip-scramble
pmiRZip-130b
pCDH-hNR2F6
pCDH-hSGMS1
GFP chimerism (%)
BM
Spleen
Liver
PB
Lung
D
Lineage output in BM (rescue mice)
MII-AF4+ pMIRH-130b
% of GFP+ CD45.2+ cells
Mixed
Myeloid
Control
pmiRZip 130b
pCDH hNR2F6
pCDH hSGMS1
E
Survival curve (rescue mice - microRNA inhibitor)
MII-AF4+ pMIRH-128a
Control
pmiRZip-128a
pmiRZip-130b
pmiRZip-128a + 130b
3 leukemic/6 total
Median survival
61 days
3 leukemic/5 total
Median survival
56 days
3 leukemic/3 total
Median survival
36 days
7 leukemic/7 total
Median survival
36 days
Percent survival
Time (days post-transplant)
F
Survival curve (rescue mice - NR2F6 and SGMS1)
MII-AF4+ pMIRH-128a
Control
pCDH-hNR2F6
pCDH-hSGMS1
0 leukemic/4 total (stroke)
Median survival
34 days
p = 0.08
3 leukemic/4 total
Median survival
45 days
3 leukemic/3 total
Median survival
36 days
Percent survival
Time (days post-transplant)
G
GFP chimerism in BM (rescue mice)
MII-AF4+ pMIRH-128a
GFP chimerism (%)
NS
Control
pmiRZip 128a
pmiRZip 130b
pmiRZip 128a 130b
pCDH hNR2F6
pCDH hSGMS1
H
MII-AF4+ pMIRH-128a Control
MII-AF4+ pMIRH-128a pmiRZip-128a
MII-AF4+ pMIRH-128a pmiRZip-130b
Spleen
Liver
Femur/ tibia
MII-AF4+ pMIRH-128a pmiRZip-128a + 130b
MII-AF4+ pMIRH-128a pCDH-hNR2F6
MII-AF4+ pMIRH-128a pCDH-hSGMS1
I
Apoptosis (rescue mice)
Bone marrow
Necrosis
Late apoptosis
Early apoptosis
% of GFP+ CD45.2+ Singlets
Control mice
pCDH hNR2F6
pCDH hSGMS1
pCDH hNR2F6
pCDH hSGMS1
MII-AF4+ pMIRH-130b
MII-AF4+ pMIRH-128a